Supplemental material to this article can be found at:
http://molpharm.aspetjournals.org/content/suppl/2022/05/23/molpharm.121.000430.DC1
1521-0111/102/1/1–16$35.00
MOLECULAR PHARMACOLOGY
dx.doi.org/10.1124/molpharm.121.000430
Mol Pharmacol 102:1–16, July 2022

Physiologic Targets and Modes of Action for CBL0137, a Lead for Human African Trypanosomiasis Drug Development[S]

Carlos E. Sanz-Rodríguez, Benjamin Hoffman, Paul J. Guyett, Andrei Purmal, Baljinder Singh, Michael P. Pollastri, and Kojo Mensa-Wilmot

Department of Cellular Biology, University of Georgia, Athens, Georgia (C.E.S.-R., B.H., P.J.G., K.M.-W.); Buffalo Biolabs Inc, Buffalo, New York (A.P.); Department of Chemistry and Chemical Biology, Northeastern University, Boston, Massachusetts (B.S., M.P.); and Department of Molecular and Cellular Biology, Kennesaw State University, Kennesaw, Georgia (K.M.-W.)

Received October 10, 2021; accepted April 20, 2022

ABSTRACT

CBL0137 is a lead drug for human African trypanosomiasis, caused by *Trypanosoma brucei*. Herein, we use a four-step strategy to 1) identify physiologic targets and 2) determine modes of molecular action of CBL0137 in the trypanosome. First, we identified fourteen CBL0137-binding proteins using affinity chromatography. Second, we developed hypotheses of molecular modes of action, using predicted functions of CBL0137-binding proteins as guides. Third, we documented effects of CBL0137 on molecular pathways in the trypanosome. Fourth, we identified physiologic targets of the drug by knocking down genes encoding CBL0137-binding proteins and comparing their molecular effects to those obtained when trypanosomes were treated with CBL0137. CBL0137-binding proteins included glycolysis enzymes (aldolase, glyceraldehyde-3-phosphate dehydrogenase, phosphofructokinase, phosphoglycerate kinase) and DNA-binding proteins [universal minicircle sequence binding protein 2, replication protein A1 (RPA1), replication protein A2 (RPA2)]. In chemical biology studies, CBL0137 did not reduce ATP level in the trypanosome, ruling out glycolysis enzymes as crucial targets for the drug. Thus, many CBL0137-binding proteins are not physiologic targets of the drug. CBL0137 inhibited 1) nucleus mitosis, 2) nuclear DNA replication, and 3) polypeptide synthesis as the first carbazole inhibitor of eukaryote translation. RNA interference (RNAi) against RPA1 inhibited both DNA synthesis and mitosis, whereas RPA2 knockdown inhibited mitosis, consistent with both proteins being physiologic targets of CBL0137. Principles used here to distinguish drug-binding proteins from physiologic targets of CBL0137 can be deployed with different drugs in other biologic systems.

SIGNIFICANCE STATEMENT

To distinguish drug-binding proteins from physiologic targets in the African trypanosome, we devised and executed a multidisciplinary approach involving biochemical, genetic, cell, and chemical biology experiments. The strategy we employed can be used for drugs in other biological systems.

Introduction

Human African trypanosomiasis (HAT) is caused by *Trypanosoma brucei gambiense* and *T.b. rhodesiense*. Being a zoonotic disease transmitted by tsetse flies, a reservoir of *T. brucei* in nonhuman vertebrates in the wild is a significant problem for elimination. HAT is managed with chemotherapy: Fexinidazole, the first new drug in 50 years, was approved in 2018 for treatment of HAT caused by *T. b. gambiense* (Pollastri, 2018; Watson et al., 2019; Lindner et al., 2020). Limitations of current medications call for continued work to discover new drugs. In the case of fexinidazole, patients' noncompliance is an issue because of nausea and vomiting. Further, recrudescence of HAT is reported after treatment (Sokolova et al., 2010; Pelfrene et al., 2019). Thus, there is need to find new drugs against HAT, but only one drug, acoziborole (SCYX-7158), is currently in clinical trials (Jacobs et al., 2011; Jones et al., 2015).

Phenotypic (i.e., whole-cell) screening has made important contributions to discovery of hits for infectious diseases (Swinney and Anthony, 2011; Butera, 2013; Ferguson et al., 2019; Patra et al., 2020). In antiparasite drug development, there is significant evidence for prominence of "phenotypic screening" in drug discovery (Buckner et al., 2020): SCYX-7158 entered phase 2 clinical trials for HAT without knowledge of its target (Thomas et al., 2016), and only recently have "modes of action" studies received attention (Torreele et al., 2010; Kaiser et al., 2011; Koman et al., 2012). Phenotypic screening is also important for discovering hits against some cancers and neurologic and chronic diseases(Abo-Rady et al., 2019; Bryce

This work was supported by National Institutes of Health National Institute of Allergy and Infectious Disease [Grant R01-AI126311] and [Grant R01-AI124046] (to K.M.-W.).
No author has an actual or perceived conflict of interest with the contents of this article
dx.doi.org/10.1124/molpharm.121.000430.

[S] This article has supplemental material available at molpharm.aspetjournals.org.

ABBREVIATIONS: 1K0N, anucleate; 2K1N, two kinetoplasts and one nucleus; DAPI, 4',6-Diamidino-2-Phenylindole; DCC, delayed cytocidal concentration; DIC, differential interference contrast microscopy; EdU, 5-Ethynyl-2'-deoxyuridine; FU, fluorescence unit; GI, growth inhibitory; HAT, human African trypanosomiasis; HPG, L-homopropargylglycine; Intercept-PBS, PBS-based Intercept; K, kinetoplast; kDNA, kinetoplast DNA; mAb, monoclonal antibody; N, nucleus; PBS-G, PBS with 10 mM glucose; RNAi, RNA interference; RPA1, replication protein A1; RPA2, replication factor A2; SM, single marker; UMSBP2, universal minicircle sequence binding protein 2.

et al., 2019; Weng et al., 2019; Drowley et al., 2020; Ruillier et al., 2020; Swalley, 2020; Wang et al., 2020; Keatinge et al., 2021; Shapovalov et al., 2021).

Curaxins are carbazole derivatives with acyl substituents at positions 3- and 6- of the scaffold and a pendant secondary or tertiary amino group that is separated by 2-to-4 carbon atoms from the carbazole nitrogen. Curaxin CBL0137 is undergoing phase 1 clinical evaluation and is active against some human cancer cell lines. CBL0137 has several modes of action, including chromatin remodeling, in mammalian cells (Koman et al., 2012; Sergeev et al., 2020).

In antitrypanosome drug development, CBL0137 emerged as a lead drug from phenotypic screening (Thomas et al., 2016). Consequently, neither its target nor mechanism of action is known. In this study, we have attempted to find CBL0137-binding proteins in trypanosomes, using drug affinity chromatography. Fourteen CBL0137-binding proteins were discovered, and they were used to develop hypotheses regarding possible modes of antitrypanosome action of CBL0137. Next, we screened the CBL0137-binding proteins as possible physiologic targets of the drug since binding of the drug to many proteins may have no biologically significant effects in vivo. For example, plasma proteins bind drugs but are not considered physiologic targets of the small molecules. A "physiological target of a drug" may be defined as a gene whose knockdown (or over-expression) yields very similar/identical molecular effects as treatment of cells with the drug. Genes encoding CBL0137-binding proteins were knocked down and the molecular effects compared with those obtained from perturbation of trypanosomes with the drug. The expectation was that when a physiologic target was knocked down, the molecular defects reported would be very similar to those obtained when the drug was added to trypanosomes. The principle of expecting a drug to "phenocopy" knockdown of its physiologic target has been established by the Shapiro (Meyer and Shapiro, 2021) and Mensa-Wilmot laboratories (Guyett et al., 2016).

Our systematic and multidisciplinary strategy revealed concentration-dependent selectivity in modes of action for the drug. CBL0137 inhibited both nuclear DNA replication and nucleus segregation (i.e., mitosis) at low concentrations (less than 180 nM). At higher concentration (i.e., above 280 nM), the drug blocked protein synthesis. Of fourteen CBL0137-binding proteins documented, data obtained for replication protein A1 (RPA1) and replication protein A2 (RPA2) are consistent them being physiologic targets of CBL0137. We concluded that CBL0137 is a multitarget drug that affects three biologic pathways (DNA replication, synthesis of proteins, and nucleus segregation) in the African trypanosome.

Methods

Cell and Culture Conditions. Bloodstream *T. brucei* Lister 427, single marker (SM) (Wirtz et al., 1999), and specific trypanosome lines for RNA interference (RNAi) (RPA1-RNAi, RPA2-RNAi, universal minicircle sequence binding protein 2 (UMSBP2)-RNAi, and eIF4A1-RNAi (Supplemental Material) were cultured in HMI-9 medium (Hirumi and Hirumi, 1989) supplemented with 10% tetracycline-free fetal bovine serum (Atlanta Biologicals, Flowery Branch, GA) and 10% Serum Plus (Sigma-Aldrich) at 37°C, 5% CO_2 (primers used for preparation of RNAi constructs are described in Supplemental Table 2). Antibiotics for parasite maintenance of stable trypanosome lines were hygromycin (5 μg/ml), G418 (6.4 μg/ml), puromycin (0.5 μg/ml), and blasticidin (5 μg/ml).

Delayed Cidality Assays. Parasites (10^3 cells per milliliter or 10^5 cells per milliliter) were incubated with different concentrations of CBL0137 or DMSO (0.1%) for 6 hours. Then, cells were washed, resuspended in fresh medium at 10^4 trypanosomes per ml, and incubated for 48 hours. Trypanosomes were enumerated with a Coulter-Counter (Beckman).

5-Ethynyl-2'-deoxyuridine (EdU) assays. Bloodstream trypanosomes (5×10^5 cells per milliliter) were preincubated for 15 minutes with different concentrations of the drugs (in HMI-9 medium), EdU (Abcam) was added to 300 μM (final concentration), and cells were incubated for 1 hour. Cells were prepared as previously described (Sullenberger et al., 2017). Images of trypanosomes were captured using a DeltaVision II Olympus inverted microscope (Fig. 2) or Keyence BZ-X800 (Fig. 9), and data were processed with Fiji (ImageJ, v 2.0.0). Images were masked in the nuclei area, and the pixel intensity for each image was stretched until getting the entire intensity range. Finally, all pixel values were added (integrated), and the resulting value, named integrated intensity, was plotted. Data for integrated intensity was processed using CellProfiler 3.1.9 (McQuin et al., 2018).

Protein Synthesis Assay. Trypanosomes were cultured to late log phase (between 2×10^5/ml and 1×10^6/ml). Cells were harvested, washed, and resuspended (5×10^5 cells per milliliter) in RPMI without methionine, supplemented with 10% fetal bovine serum and incubated for 15 minutes with different concentrations of drugs. L-Homopropargylglycine (HPG) (Cayman Chemical) was added (to 4 μM), followed by incubation for 1 hour at room temperature. Cells were harvested, washed with PBS-G (PBS with 10 mM glucose), pelleted ($\sim 5 \times 10^6$ cells), and resuspended in 50 μl of permeabilization buffer (50 mM HEPES pH 7.4, 0.025% NP-40) on ice for 30 minutes. Fifty microliters of "click-chemistry" cocktail (20 mM Tris buffer, pH 7.4, 5 mM CuSO4, 300 mM ascorbic acid, 140 mM NaCl, and 17.5 μM azide-PEG3-biotin) was added, and the mixture was incubated at room temperature for 1 hour. Proteins were precipitated by adding 400 μl of ice-cold acetone, pelleted (4°C, 20 minutes, 20,000*g*), dried, and resuspended in SDS sample buffer (1×10^5 cells per microliter). Proteins were heated at 95°C for 5 minutes, separated by SDS-PAGE (12%), transferred onto low-fluorescence polyvinylidene fluoride (PVDF) membrane (Bio-Rad), and developed with streptavidin-IRDye 800CW (Li-COR) (1:2500 dilution). Images were captured with an Odyssey CLx imaging system (Li-Cor), and data were processed using Empiria Studio Software (Li-Cor).

Preparation of Curaxin-Agarose Drug Affinity Column. The preparation of the alkyne derivative of CBL0137 (Table 1) is reported in the Supplemental Material (Supplemental Scheme 1 and 2). This compound was coupled to azide agarose beads using copper-catalyzed click chemistry (Rostovtsev et al., 2002; Punna et al., 2005), following recommendations in a tris-hydroxypropyltriazolylmethylamine–based click kit (Jena Biosciences). Azide agarose beads (125 μl settled bed volume) (Jena Bioscience CLK-1038-2) were mixed with 0.5% DMSO (negative control) or alkyne derivative of CBL0137 (10 mM) in the presence of $CuSO_4$ (2 mM), tris-hydroxypropyltriazolylmethylamine (10 mM), and sodium ascorbate (100 mM in sodium phosphate buffer, pH 7.2). The beads were vortexed, incubated on a rotary mixer for 2 hours at room temperature, and washed twice with 200 μl PBS for 20 minutes before use.

TABLE 1
Proteins that bind a curaxin-affinity column
Proteins in a trypanosome lysate were adsorbed to curaxin-agarose beads (see *Materials and Methods*). After washing with PBS, proteins bound to the affinity column were eluted with buffer containing CBL0137 (50 μM) and identified by mass spectrometry (*Materials and Methods*). The table presents proteins identified after mass spectrometry of eluates from the curaxin-affinity column. A posterior error probability value [the probability that the peptide spectrum match (PSM) is incorrect (Käll et al., 2008; Käll et al., 2009)] was calculated in Proteome Discoverer (Orsburn, 2021; Palomba et al., 2021).

Gene ID	Description	Peptide Sequences Identified in TritrypDB	N of Times Peptide Was Identified	PEP Value	Spectral Counts	
					Azide Agarose Bead (Control) Average	Curaxin Affinity Beads Average
Metabolic enzymes						
Tb427.10.5620	Fructose-bisphosphate aldolase	TDCGLEPLVEGAK	3	1.67×10^{-3}	15.7 ± 4.0	34.3 ± 7.5
Tb427.06.4280	Glyceraldehyde-3-phosphate dehydrogenase	NPADLPWGK	2	1.82×10^{-2}	7.0 ± 4.0	16.0 ± 1.7
Tb427.03.3270	ATP-dependent phosphofructokinase	TIDNDLSFSHR	3	2.3×10^{-3}	5.7 ± 2.1	15.3 ± 1.5
Tb427.01.700	Phosphoglycerate kinase	VDFNVPVK	2	5.7×10^{-2}		4.0 ± 1.0
Tb427.08.6390	lysophospholipase	FLQQVLPGPSSK	1	4.3×10^{-3}		3.5 ± 2.1
Tb427.10.16120	Inosine-5′-monophosphate dehydrogenase	GISGILVTEGGK	1	1.95×10^{-2}		3.5 ± 2.1
DNA-associated proteins						
Tb427.10.6060	Universal minicircle sequence binding protein 2	ACYHCQQEGHIAR	3	2.4×10^{-4}		11.7 ± 8.7
Tb427.05.1700	Replication protein A 28 kDa subunit	ITDGTGVVVVR	3	2.6×10^{-3}		4.3 ± 3.2
Tb427tmp.01.0870	Replication protein A1	VKEEGLGGNEDSER	2	3.3×10^{-4}	3.3 ± 3.2	
RNA-associated proteins						
Tb427tmp.211.2150	Poly(A)-binding protein 2	NFDDTVTSER	3	6.6×10^{-3}		11.7 ± 3.5
Tb427.04.2040	ALBA-domain protein	SAVGVAEVLK	3	2.4×10^{-3}		7.3 ± 1.5
Tb427tmp.211.4540	RNA-binding protein DRBD2	ETFQQVGEVER	2	2.9×10^{-2}		4.7 ± 2.5
Tb427tmp.211.0560	RNA-binding protein DRBD3	NNEIGEVSR	2	5.3×10^{-3}		3.5 ± 3.5
Tb427tmp.160.3270	Eukaryotic initiation factor 4A-1	GGDIIAQAQSGTGK	2	1.9×10^{-3}	2.0	2.5 ± 0.7

PEP, posterior error probability.

Affinity Chromatography with Curaxin Class 3 Agarose. *T. brucei* Lister 427 were axenically cultured in HMI-9 medium to a density of 10^6 cells per milliliter, harvested, and washed in cold PBS-G. Cells (10^8) were resuspended in 1 ml of lysis buffer [50 mM sodium phosphate, pH 7.2; 100 mM NaCl, 0.1% NP-40, 5% glycerol, and Halt Protease Inhibitor Cocktail (Thermofisher)]. Trypanosomes were sonicated in an ice bath with a QSonica, LCC sonicator, model Q55 at amplitude set to 45, 3 cycles of "30 seconds on and 2 minutes off." Sonicated mixture was diluted twofold with cold PBS, and 100 μl of precleared (12,000g, 5 minute, 4° C) lysate (10^8 trypanosome equivalent) was applied to curaxin-agarose (100 μL) or to an equivalent volume of agarose beads (negative control). The lysate was incubated with the beads at 4°C overnight and washed with 500 μL of cold PBS five times. Bound proteins were eluted by incubating beads with 200 μL PBS containing CBL0137 (50 μM) for 1 hour, 4°C. Eluted proteins were resolved by SDS-PAGE (12%) and stained with Pierce Silver for Mass Spectrometry kit (Pierce) to visualize polypeptide bands.

Mass Spectrometry Analysis. Proteins from curaxin-affinity column or agarose beads were extracted from the gel and prepared for mass spectrometry as described previously (Guyett et al., 2016). Tryptic peptides were purified using the C18 column (ZipTip) (Millipore Corporation) and divided into two technical replicates for liquid chromatography-tandem mass spectrometry (LC-MS/MS) analysis on an Easy-nLC 1000 (Thermo Scientific) coupled to an Orbitrap Fusion mass spectrometer (Thermo Scientific). LC-MS/MS run conditions were used as previously described (Guyett et al., 2016). The mass spectrometer was operated in a data-dependent tandem mass spectrometry (MS/MS) mode. The most abundant ions from the precursor scan were selected for MS/MS analysis using high-energy collisional dissociation and analyzed with an ion trap. Data from technical replicates were combined, analyzed using Proteome Discoverer 2.0 (ThermoScientific), and searched with SEAQUEST (Eng et al., 1994) against a *T. brucei* database (tritrypdb.org) that included common contaminants. Trypsin was set as the protease with maximum missed cleavages fixed at two. The precursor ion tolerance was set to 10 ppm, and the fragment ion tolerance was set to 0.6 Da. Variable modifications were methionine oxidation (15.995 Da) and phosphorylation (79.966) on serine, threonine, and tyrosine. Search results were run through Percolator (Käll et al., 2007) for scoring. Results were filtered for peptides with a false discovery rate of 0.05. The number of peptide spectrum matches (spectral counts) for each protein were obtained in three independent experiments. Posterior error probability (PEP) values for each peptide were calculated in Proteome Discoverer 2.0 (ThermoScientific).

Antibodies. Antibodies (named) were used at the following dilutions: YL1/2 (EMD Millipore; Billerica, MA) against TbRP2 (Andre et al., 2014) at 1:2500, rabbit anti-V5 (D3H8Q) (Cell Signaling; Danvers, MA) at 1:1000 for immunofluorescence and 1:3000 for western blotting, and anti-Myc mouse monoclonal (9E10) (Santa Cruz) at 1:2000 for western blots. Secondary antibodies for immunofluorescence were conjugated

to either Alexa Fluor-488 (AF-488) or AF-594 (Invitrogen) and were used at 1:3000 dilution. Anti-mouse or anti-rabbit IRDye secondary antibodies 800CW (Li-Cor, Lincoln, NE) were used for western blots at 1:20000 dilution. Epitope-tagging of trypanosomes (Shen et al., 2001) was performed with primers presented in Supplemental Methods (Supplemental Table 3).

Immunofluorescence. Trypanosomes were pelleted by centrifugation, rinsed once with PBS-G, fixed with paraformaldehyde (4% in PBS) for 20 minutes, and applied to a coverslip precoated with poly-L-lysine. The coverslip was rinsed in PBS and then in 100 mM NH_4Cl/100 mM glycine for 10 minutes to quench the fixation of cells. Trypanosomes were rinsed thrice with PBS, 5 minutes each time, and incubated for 1 hour with a "blocking and permeabilizing solution" [PBS, fish-gelatin (1X; Biotium), 1% bovine serum albumin, 0.1% Tween-20]. Primary antibody was added for an hour, after which the coverslip was rinsed thrice with PBS (as described earlier). Secondary antibody was then incubated with the coverslips in the blocking for 1 hour, rinsed three times with PBS, and then mounted on slides in Vectashield containing 4',6-Diamidino-2-Phenylindole (DAPI) (5μM) for image acquisition.

Western Blotting. Trypanosomes were collected by centrifugation and washed with PBS-G. Cells were lysate by direct resuspension in SDS sample buffer plus 1 mM of β-mercaptoethanol with final density of 1×10^5 or 3×10^5 of cells per microliter and boiled for 5 minutes at 95°C. Ten microliters of sample was loaded in each lane (1–3 × 10^6 cell equivalents per sample). Proteins were separated on TGX Fast-Cast acrylamide (12%) gel (Bio-Rad, Hercules, CA) and transferred to Low-Fluorescence polyvinylidene difluoride membrane using a Trans-Blot Turbo system (Bio-Rad). The membrane was treated with Revert Total Protein Stain for WB (LI COR, Lincoln, NE) in PBS-based Intercept (Intercept-PBS) blocking solution. Primary antibody was added in Intercept-PBS/0.2% of Tween-20. Secondary antibody was used in Intercept-PBS/0.2% Tween-20/0.01% of SDS. Empiria Studio Software (LI COR) was used to measure the intensity of the secondary antibody signal (at 800 nm) for each antigen. For each lane, normalization was carried out in Empiria Studio Software using a density integrity over the entire lane for each condition obtained at 700 nm (for Revert total protein stain). Western blots were performed in triplicate, and the normalized bands in each sample lane were averaged.

Quantitation of Total Protein in Western Blots. Cultures of a clonal line of *T. brucei* stably transfected with V5-NRP1 (1×10^5 cells per milliliter) were incubated with or without DMSO, or CBL0137 (730 nM) for 6 hours in HMI-9 medium, lysed, and separated (1×10^6 trypanosome equivalents per lane) in a TGX Fast-Cast Stain-free acrylamide (12%) gel (see section directly above). Images were acquired with a ChemiDoc XRS+ (Bio-Rad). The experiment was performed thrice with different biologic samples. Values for total fluorescence in each lane were obtained using Fiji (ImageJ, v 2.0.0). To determine possible statistical significance of differences in total fluorescence per lane, a paired two-sided t test (in Graphpad Prism 9.0) was used [a representative image for gel from one experiment is presented Fig. 7B (lower panel, center)].

Statistical Analysis. For noncategorical data with few points, we implemented a two-sided paired Student's t test or paired one-way ANOVA. A two-sided Kolmogorov-Smirnov test was employed for data with a wide range and whose distribution was not normal to test for significance of differences in the distribution. When distribution of distinct types of trypanosomes (categorical data) was analyzed, a χ^2 test was used to test for differences in distributions between different groups. All analyses were executed with GraphPad Prism 9.0. For all analysis, $\alpha = 0.05$.

Results

Determination of Pharmacodynamically Equivalent Concentrations of Drugs. Major goals of our work were to 1) determine mechanisms of action of CBL0137 against trypanosome and 2) identify proteins that interacted with the drug. Since we planned to study control compounds, it was important to decide the concentration of each drug for each experiment. Here, we avoided using identical concentrations of drugs (per experiment) since their varying physicochemical properties result in nonequivalent quantities accumulating in trypanosomes. Given these considerations, we used an empirically determined drug concentration termed "delayed cidal concentration" (DCC) whose "readout" was relative trypanocidality. DCC assays (described below) are performed by treating cells for a short period with drugs and washing the drug off. The trypanosomes are viable immediately after treatment with the drug (monitored by permeability to propidium iodide); cidality is determined after culturing drug-treated cells for 48 hours.

Experimentally, we determined DCC by treating trypanosomes (10^5/ml in culture medium) with varying concentrations of a drug for 6 hours (Fig. 1). After washing the drug off, cells were resuspended in a fresh medium and cultured for 48 hours, and trypanosome density was quantitated. The concentration of drug that caused 25%, 50%, or 90% cidality, in comparison with DMSO-treated control trypanosomes, was termed DCC_{25}, DCC_{50}, and DCC_{90}, respectively (Fig. 1; Supplemental Table 1). DCC_{25}, for example, permits us to study early molecular effects of a drug on trypanosomes before cidal effects manifest.

For different drugs, DCC_{25} determined with a fixed inoculum of cells (e.g., 5×10^5/ml) varied dramatically. For example, for CBL0137 and cycloheximide, DCC_{25} values were 180 nM and 2840 nM, respectively (Supplemental Table 1). These data are consistent with our suspicion that differences in drug properties affect concentrations needed for equivalent trypanocidality. Thus, DCC's represent pharmacodynamically equivalent amounts of drug. To determine modes of action of hits, we used DCC_{25} amounts for each drug in our studies.

In a parallel set of experiments, we determined drug concentrations required to limit proliferation (instead of cidality) of trypanosomes (1×10^5/ml) in 6 hours by 25%. For CBL0137, concentrations for growth inhibition by 25%, 50%, and 90% were 290 nM, 590 nM, and 2540 nM, respectively. Thus, in each case, GI concentration was higher than the corresponding DCC. These data suggest that it is preferable to use DCC amounts of drug to study biologic effects of curaxins because they are consistently lower than GI concentrations. Biologic effects of drugs are best studied with the smallest nontoxic concentrations that can be used.

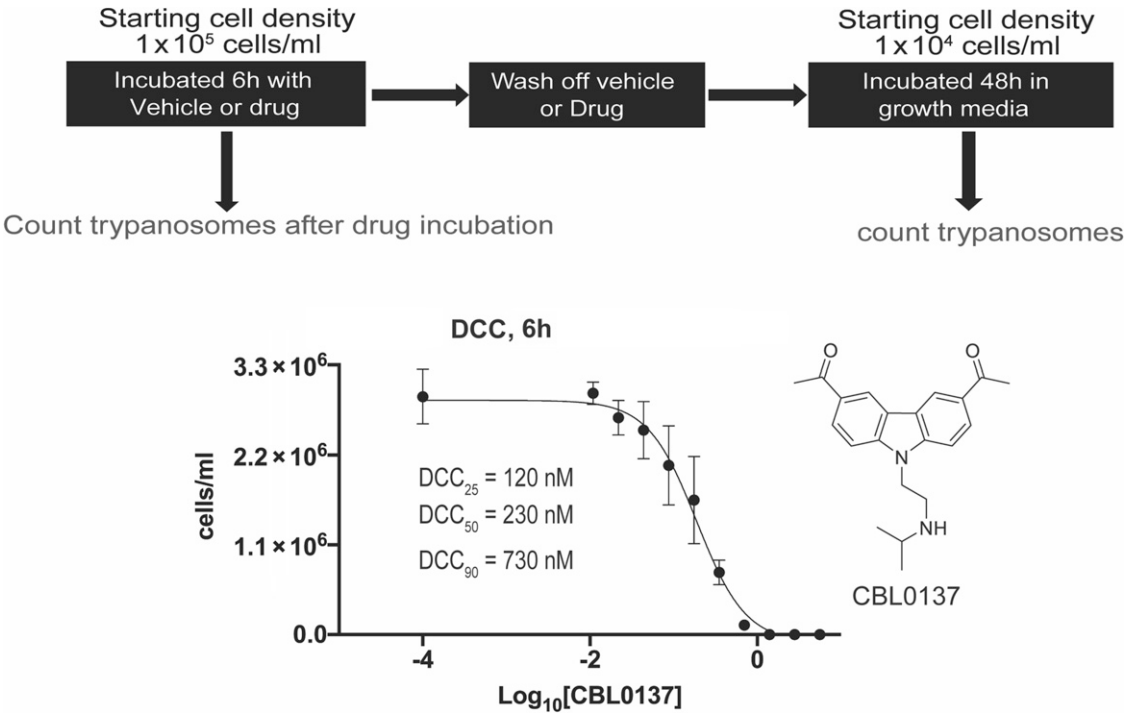

Fig. 1. Delayed cidal concentration of CBL0137. *T. brucei* (1×10^5 cells per milliliter) was incubated with different concentrations of CBL0137 or DMSO (0.1%) for 6 hours. Cell density was obtained with a Coulter counter. Cells were rinsed and transferred to fresh drug-free HMI-9 medium at a density of 1×10^4 cells per milliliter and cultured at 37°C for 48 hours. Trypanosomes were enumerated in a Coulter counter or hemocytometer after 48 hours. Curves were fit to data points using a nonlinear function [log (inhibitor) versus response – variable slope for four parameters] in Prism 9.0 (Graphpad). Bars indicate mean and S.D.

Identification of CBL0137-Binding Proteins and Prediction of Biologic Effects of CBL0137 on Bloodstream *T. brucei*

Drug-binding proteins can provide clues about the modes of action of small molecules. For that reason, we searched for trypanosome proteins that associate with CBL0137 using affinity chromatography. In our protocol, proteins from a trypanosome lysate were retained by a drug-agarose column (Fig. 2). Following several washes with PBS buffer, proteins were eluted with buffer containing CBL0137 (50 μM), and they were identified by liquid chromatography–mass spectrometry (Table 1). As a control, the trypanosome lysate was loaded on a column of azide agarose, from which bound proteins were eluted with CBL0137 (Table 1). The experiment was performed thrice. Data were filtered for peptides with a false discovery rate of 0.05, and the number of spectral counts for each protein was determined in the three independent experiments.

Four enzymes in the glycolysis pathway (fructose-bisphosphate aldolase, glyceraldehyde-3-phosphate dehydrogenase, phosphofructokinase, and phosphoglycerate kinase) were retained by the drug-affinity column (Table 1). As a result, we evaluated the possibility that CBL0137 affected ATP homeostasis since this nucleoside triphosphate is produced predominantly from glycolysis in bloodstream *T. brucei* (Van Weelden et al., 2003; Schnaufer et al., 2005; Brown et al., 2006). CBL0137 did not affect cytosolic ATP levels, whereas control 2-deoxyglucose depleted the nucleotide (Supplemental Fig. 1). We infer that CBL0137, although it binds to some glycolytic enzymes (Table 1), is unlikely to inhibit their activity.

DNA-binding proteins RPA1, RPA2, and UMSBP2 were eluted with CBL0137 from the drug-affinity column (Table 1). Homologs of RPA1 and RPA2 are part of a heterotrimeric complex involved in DNA synthesis and damage response in other eukaryotes (Bochkarev et al., 1999; Kim and Brill, 2001; Olson et al., 2006; Haring et al., 2008; Han et al., 2018). In *T. brucei,* RPA2 is associated with nuclear DNA (Glover et al., 2019). Based on these facts, we hypothesized that CBL0137 might affect DNA replication and/or a DNA repair response.

CBL0137 Inhibits DNA Synthesis and Nucleus Mitosis. We tracked DNA replication in bloodstream *T. brucei* by monitoring incorporation of the thymidine analog EdU into nuclear DNA. The effect of CBL0137 on DNA replication was assessed by preincubating trypanosomes with the drug for 15 minutes before the addition of EdU for 1 hour (Fig. 3). In the absence of the drug, robust DNA replication was documented in nuclei (Fig. 3A). CBL0137 (180 nM) inhibited EdU incorporation into nuclei; median fluorescence dropped from 433 fluorescence units (FU) to 333.4 FU ($P = 2.2 \times 10$ by Kolmogorov-Smirnov test) (Fig. 3B). Higher amounts of CBL0137, DCC_{50} (290 nM), and DCC_{90} (800 nM) further reduced median nuclear fluorescence to 152.7 FU and 82.3 FU, respectively ($P = 4.0 \times 10^{-6}$, and $P < 1 \times 10^{-15}$, respectively) (Fig. 3B).

As control, we checked whether the synthesis of mitochondrial DNA [termed kinetoplast DNA (kDNA)] was affected by CBL0137. CBL0137 did not inhibit the replication of kDNA (Fig. 3C). So, we conclude that CBL0137 selectively inhibits nuclear DNA synthesis in *T. brucei*.

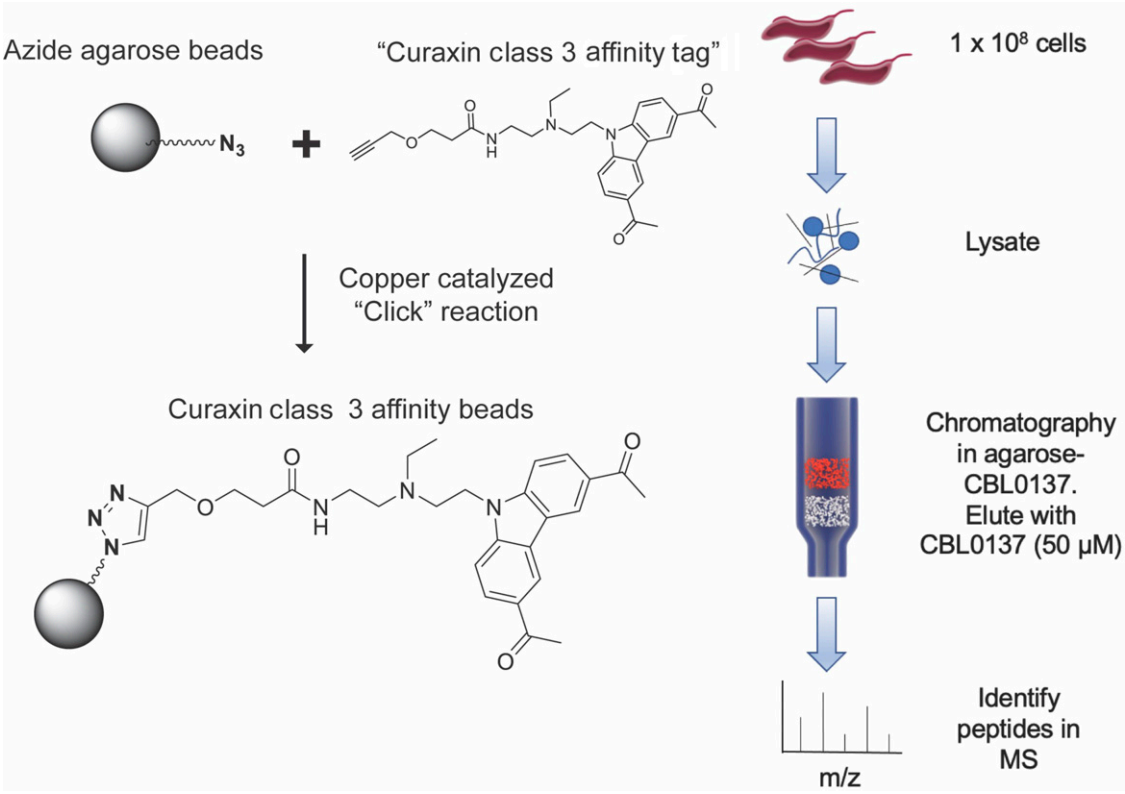

Fig. 2. Affinity chromatography and identification of CBL0137-binding proteins.

We reported in an earlier study that long-term exposure of trypanosomes to CBL0137 prevented mitosis of the nucleus (Thomas et al., 2016). For that reason, we wanted to learn whether short-term exposure of trypanosomes to CBL0137 prevented mitosis. To test whether limited exposure of trypanosomes to CBL0137 affected mitosis, we treated cells (5×10^5/ml) with DCC_{25} (180 nM), DCC_{50} (290 nM), or DCC_{90} (800 nM) drug for 6 hours (Fig. 4) and then analyzed the data. Trypanosomes with two kinetoplasts and one nucleus (2K1N) accumulated after the 6-hour treatment with CBL0137, and the fraction of 2K1N cells increased for DCC_{50} (290 nM) as well as DCC_{90} (800 nM) (Fig. 4). These data indicate that inhibition of mitosis is a major effect of short-term treatment of bloodstream *T. brucei* with CBL0137.

RPA1 and RPA2 Are Physiologic Targets of CBL0137. CBL0137 binds to multiple proteins (Table 1), many of which may not be the basis of the drug's mode of action in a trypanosome. Physiologic targets are a subset of drug-binding proteins whose genetic knockdown (or overexpression in some cases) produces molecular effects similar to those obtained when the drug is added to cells (Mensa-Wilmot, 2021). After identifying fourteen CBL0137-binding proteins (Table 1) and learning that the drug does not block glycolysis (Supplemental Fig. 1) but inhibits DNA replication (Fig. 3), limits protein synthesis (Fig. 8), and prevents mitosis (Fig. 4), we searched for physiologic targets of the drug.

Since CBL0137 inhibited nuclear DNA replication (Fig. 3), we were interested in a CBL0137-binding protein whose knockdown reduced DNA synthesis in the nucleus as a possible physiologic target of the drug. RPA1 is a single-stranded DNA-binding protein that is important for synthesis of DNA in other biologic systems (Erdile et al., 1991; Braun et al., 1997; Maniar et al., 1997; Mondal and Bhattacherjee, 2020) and other aspects of DNA metabolism (reviewed in (Wold, 1997)). Trypanosome RPA1 is bound to CBL0137 (Table 1), so we checked whether knockdown of RPA1 inhibited nuclear DNA synthesis. Toward this objective, TbRPA1 was first tagged with a V5 epitope in a cell line where knockdown of the gene could be induced with RNA interference. RPA1 was knocked down (Fig. 5A), resulting in a 2.5-fold reduction in protein level in an immunofluorescence assay (Fig. 5B) ($P = 4.1 \times 10^{-5}$). A control basal body protein TbRP2 was unaffected by RNAi of RPAi (Fig. 5C). Knockdown of RPA1 was confirmed by western blotting (Supplemental Fig. 3A; Supplemental Fig. 4B) showing a sevenfold reduction in protein amount (Supplemental Fig. 3B) ($P = 0.029$). A trypanosome proliferation defect was observed beginning 12 hours after RNAi induction (Supplemental Fig. 3C).

Regarding DNA replication, the fraction of EdU^+ trypanosomes decreased fourfold ($P = 1.8 \times 10^{-3}$) after the knockdown of RPA1 (Fig. 5E). Further, in the EdU^+ population, the amount of nucleotide analog incorporated decreased 350% ($P < 1 \times 10^{-15}$) (Fig. 5F) after knockdown of TbRPA1. We conclude that RPA1 is important for DNA replication in *T. brucei*.

Mitosis was inhibited after the knockdown of RPA1. The fraction of 2K1N cells increased from 10% to 30%, whereas 1K1N trypanosomes decreased from 80% to 45% (Fig. 5G). Further, we detected trypanosomes with more than one kinetoplast that had one nucleus (XK1N) that may have progressed from 2K1N trypanosomes. XK1N trypanosomes duplicate kDNA multiple times without mitosis (Fig. 5G). Similarly, long-term treatment of *T. brucei* with CBL0137 (200 nM for 24 hours) produces XK1N cells (Thomas et al.,

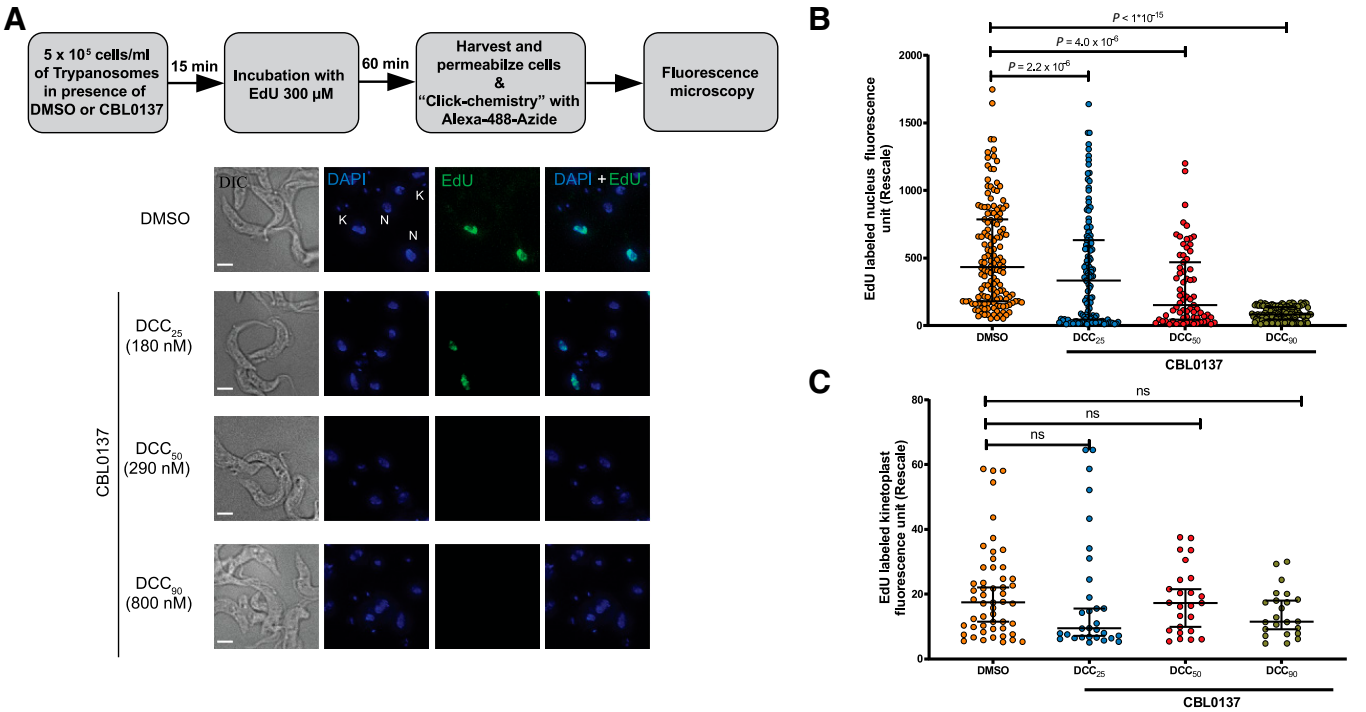

Fig. 3. Nuclear DNA synthesis is inhibited by CBL0137. (A) Scheme of the experimental protocol and representative images for trypanosomes treated as described in *Methods*. For each condition, differential interference contrast microscopy (DIC), DAPI channel (blue), EdU channel (green), and merge between DAPI and EdU are presented. Images were captured using a DeltaVision II Olympus inverted microscope, and data were processed using Fiji (ImageJ, v 2.0.0). Data for integrated intensity was processed using CellProfiler 3.1.9 (Soliman, 2015). Scale bar is 5 microns. (B) Analysis of rescaled integrated EdU fluorescence intensity in nuclei, drawn from three biologic replicates. Bars indicate median and interquartile range. Kolmogorov-Smirnov test was used to assess statistical significance of differences in distribution of fluorescence intensity between DMSO and CBL01370137 treatment groups at DCC_{25} ($P = 2.2 \times 10^{-6}$), DCC_{50} ($P = 4.0 \times 10^{-6}$), and DCC_{90} ($P < 1 \times 10^{-15}$). (C) Analysis of the rescaled integrated intensity in the kinetoplast. Bars indicate median and interquartile range. Kolmogorov-Smirnov test was used to assess statistical significance of differences in fluorescence intensity between DMSO and CBL0137 treatment groups (Soliman, 2015).

2016), in support of XK1N as a bona fide product of CBL0137 treatment of trypanosomes and affirming a conclusion that knockdown of TbRPA1 phenocopies addition of the drug to *T. brucei*.

Our data are consistent with the conclusion that RPA1 is a physiologic target of CBL0137, because knockdown of the gene phenocopies addition of the drug to *T. brucei* (Meyer and Shapiro, 2021). Trypanosome RPA is a CBL0137-binding protein (Table 1) whose knockdown inhibits DNA replication (Fig. 5F), and prevents mitosis (Fig. 5G), like results obtained after the addition of CBL0137 to *T. brucei* (Figs. 3 and 4).

RPA2 is a CBL0137-binding protein (Table 1), so we determined whether it's genetic knockdown–inhibited DNA replication, mitosis, or protein synthesis to find out whether the protein was a physiologic target of the drug. RPA2 knockdown was engineered in a trypanosome line expressing a myc-tagged version of the protein. Induction of RNAi reduced protein levels fourfold (Fig. 6A, compare lane 3 to lane 4; Fig. 6B), and proliferation of trypanosomes was reduced 24 hours after knockdown of RPA2 (Fig. 6C). The fraction of 2K1N trypanosomes rose from 10% to 20% after RNAi against RPA2 (Fig. 6D; $P = 4.87 \times 10^{-29}$), indicating that mitosis was blocked. In addition, anucleate (1K0N) trypanosomes accumulated in the population (Fig. 6D; Supplemental Fig. 4) [bloodstream trypanosomes in G1 are 1K1N; they have one kinetoplast (K) and one nucleus (N)]. Anucleate cells, also termed zoids, have a kinetoplast but lack a nucleus (1K0N). CBL0137 treatment of *T. brucei* does not produce anucleate cells (Fig. 4).

These data imply that knockdown of RPA2 protein partially phenocopies addition of CBL0137 to trypanosomes and is consistent with RPA2 as a physiologic target of CBL0137. This inference is in line with polypharmacology of the drug in *T. brucei*. Our finding that RPA2 is important for accurate partitioning of the nucleus is a novel observation.

UMSBP2 Is Not a Physiologic Target for CBL0137. UMSBP2 binds kDNA as well as telomeres of nuclear DNA (Jensen and Englund, 2012; Povelones, 2014; Klebanov-Akopyan et al., 2018). Since UMSBP2 is a CBL0137-binding protein (Table 1), we were interested in learning whether knockdown of UMSBP2 phenocopied CBL0137 by inhibiting mitosis, reducing DNA synthesis, or blocking protein synthesis, as expected for a physiologic target (Meyer and Shapiro, 2021).

UMSBP2 knockdown (Fig. 7A) reduced protein amount sixfold (Fig. 7B) and slowed proliferation after 36 hours (Fig. 7C). Phenotypically, there was a slight increase in 1K1N cells accompanied by a decrease in 2K1N cells (Fig. 7D), but the difference in distribution of cell types was not statistically significant ($P = 0.1514$). Further, this change in the distribution of cells was not reproduced in a second knockdown line. We conclude that knockdown of UMSBP2 has a minor effect on the proliferation of bloodstream *T. brucei*, unlike the situation in insect stage (procyclic) *T. brucei*, where mitosis or kDNA

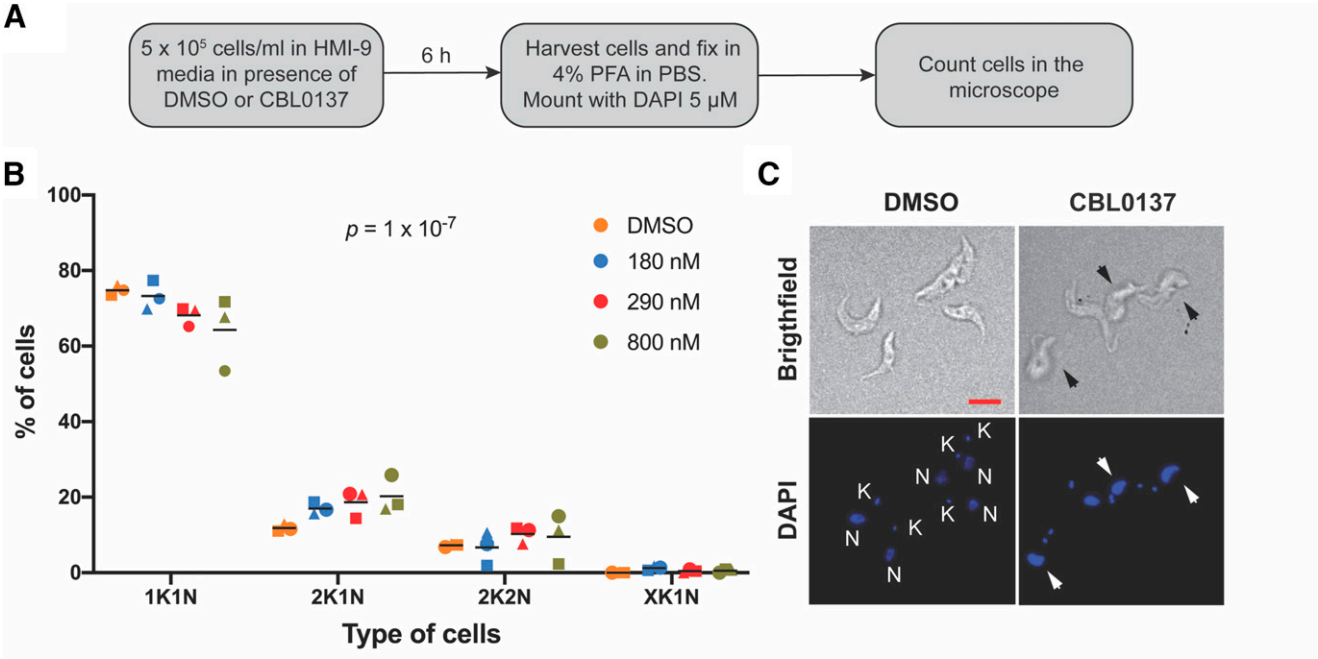

Fig. 4. CBL0137 inhibits mitosis. *T. brucei* Lister 427 (5×10^5 cells per milliliter) in HMI-9 medium were exposed to DMSO (0.1%) or CBL0137 (180 nM) at 37°C, 5% CO_2 for 6 hours. Trypanosomes were harvested and fixed in paraformaldehyde (4%) in PBS, applied to precoated coverslips with 0.01% of polylysine in PBS, and mounted in Vectashield with DAPI (5 µM). Cells were visualized using an EVOS-FL microscope (Thermofisher), and numbers of kinetoplasts and nuclei counted. (A) Experimental strategy. (B) Cell type quantitation after treatment of trypanosomes with CBL0137 (different amounts) or DMSO (vehicle for CBL0137). (C) Images (brightfield or DAPI-stained nuclei or kinetoplasts) of trypanosomes after treatment with CBL0137 (180 nM) or DMSO (solvent control). Scale bar is 5 microns. Horizontal lines represent means. Statistical significance of differences in distributions of cell types was analyzed with a χ^2 test ($P = 1 \times 10^{-7}$) using Prism 9.0 (Graphpad).

segregation were affected (Milman et al., 2007; Klebanov-Akopyan et al., 2018). In bloodstream *T. brucei*, knockdown of UMSBP2 did not inhibit mitosis (Fig. 7). Thus, although UMSBP2 is a CBL0137-binding protein (Table 1), it is not a physiologic target of the drug, because its knockdown does not phenocopy molecular effects of adding CBL0137 to trypanosomes. The caveat in interpretation of this data are the assumption that association of CBL0137 with UMSBP2 causes inhibition of the protein's activity. If CBL0137 activated UMSBP2, the appropriate study will be overexpression of the protein (discussed in Mensa-Wilmot, 2021).

Proteostasis of Epitope-Tagged Polypeptides Is Perturbed by CBL0137. Trypanosomes are not viable after a 6-hour treatment with CBL0137 (Fig. 1). From that observation, we hypothesized that CBL0137 exerted an irreversible cidal effect on bloodstream *T. brucei*. Since TbRPA1 emerged as a physiologic target of CBL0137 (see the last section), we hypothesized that exposure of *T. brucei* to CBL0137 caused irreversible loss of RPA1 protein from the cells. To test our hypothesis, we tagged RPA1 with a V5 epitope on the N-terminus, obtained stable transfectants, and treated that *T. brucei* line with CBL0137 (720 nM; DCC_{90}) for 6 hours (Fig. 8A). Cells were analyzed by western blotting for V5-RPA1 protein before and after drug exposure (Fig. 8B). Total protein in each lane was quantitated with a "stain-free" dye (see *Materials and Methods*) (Gürtler et al., 2013; Gilda and Gomes, 2015) (Fig. 8C), and that data was used to normalize the anti-V5 antibody signal (Fig. 8D).

CBL0137 reduced the amount of RPA1 by 50% (compare DMSO to CBL0137-treated samples; see lane 2 and lane 3 of Fig. 8B) after a 6-hour treatment of *T. brucei* with the drug (Fig. 8D) ($P = 2.3 \times 10^{-3}$). In a set of control experiments, we checked the effect of CBL0137 on steady-state levels of NRP1 and Tb427.03.1010 using an approach like that described for RPA1. Steady-state amounts of both NRP1 (Fig. 8B, lanes 4, 5, and 6; Fig. 8D) and Tb427.03.1010 (Fig. 8B, lanes 7, 8, and 9; Fig. 8D) decreased 50% under similar circumstances. We conclude that CBL0137 reduces steady-state amounts of V5-tagged RPA1, NRP1, and Tb427.03.1010, indicating that the effect of the drug was not limited to RPA1. Thus, CBL0137 either causes proteolysis of the three proteins in this study or triggers digestion of most trypanosome proteins (possible effects of the drug on polypeptide synthesis is addressed in the next section).

We examined a hypothesis that CBL0137 caused digestion of most proteins after trypanosome exposure to the drug. For this purpose, total protein used for western blots (Fig. 7) (10^6 cell equivalents per lane) was quantitated using TGX Fast-Cast Stain-free and fluorescence images acquired with a ChemiDoc XRS+ system (Bio-Rad) (see *Materials and Methods*) (Supplemental Fig. 6A). Differences in total protein amounts before and after CBL0137 treatment (6 hours) was not statistically significant between the two conditions (Supplemental Fig. 6B). Thus, CBL0137 does not trigger mass degradation of proteins in *T. brucei*. Instead, proteolysis induced by CBL0137 affects the three proteins that we tracked (Fig. 8). A trivial explanation for these data is that the V5 epitope on the three proteins marked them for degradation in presence of CBL0137. This hypothesis was tested by comparing three tags (V5, HA, and Myc), each appended separately to the c-terminus of a single protein TbCK1.2 (Supplemental Fig. 6C). Degradation of the three versions of TbCK1.2 was monitored as described for the proteins

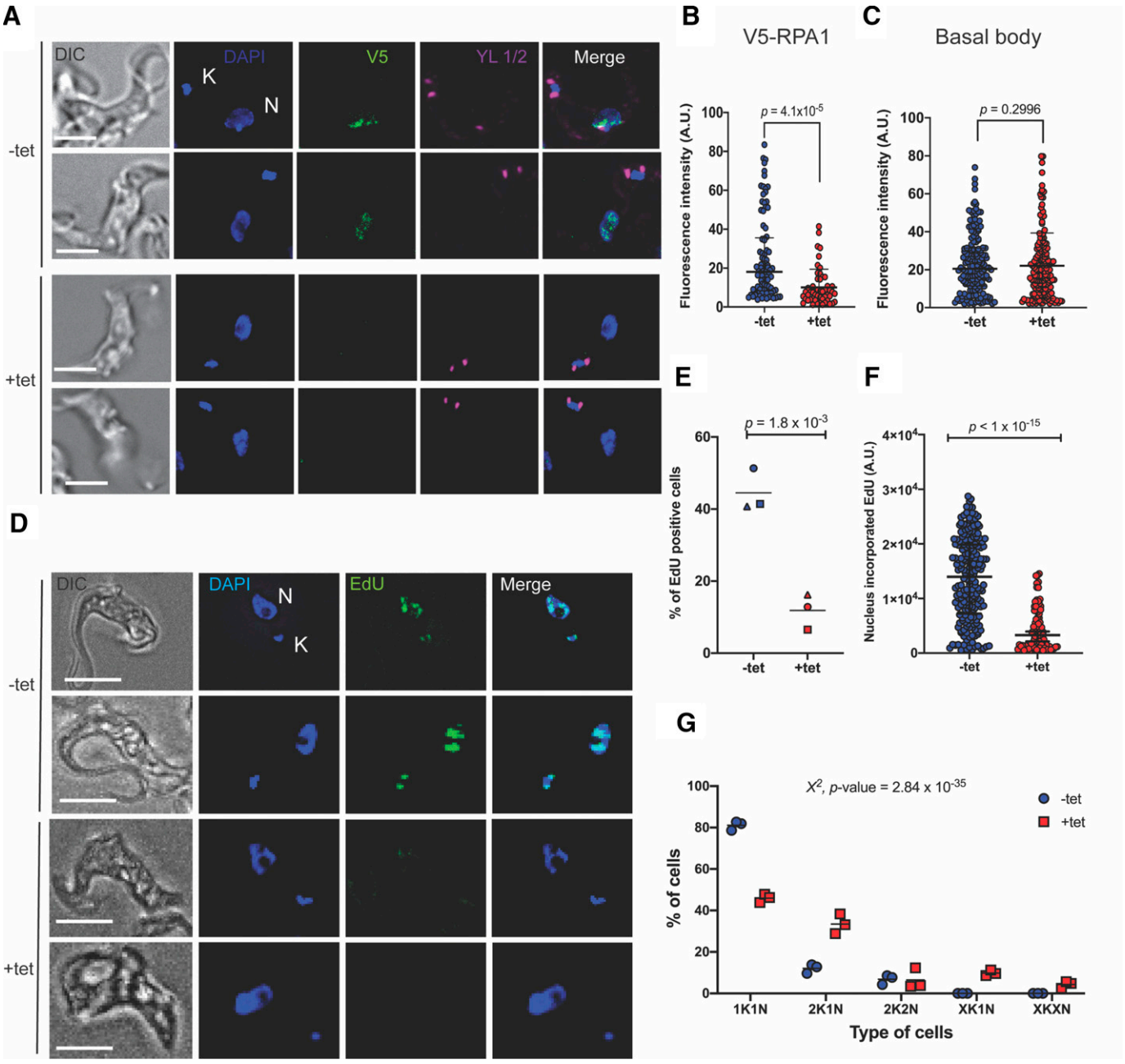

Fig. 5. RPA1 knockdown inhibits DNA replication and blocks mitosis. RNAi against RPA1 was induced for 18 hours with tetracycline (1 μg/ml). (A) Representative images for noninduced and induced RPA1 knockdown cells. DIC (first column), DAPI (blue channel), nuclear fluorescence of V5-RPA1 (green channel). Control antibody YL1/2 (recognizes basal bodies) (magenta channel). Scale bar is 5 microns. (B and C) Analysis of the fluorescence intensity of RPA1 and basal-body signals for cells induced or uninduced with tetracycline. Bars represent median and interquartile range. Kolmogorov-Smirnov test was used to assess statistical significance of differences in distribution of fluorescence data between negative and positive tetracycline treatment [$P = 4.1 \times 10^{-5}$, and $P = 0.2996$ for (B) and (C), respectively]. (D) Representative images of EdU assays for noninduced and induced cells; DIC, DAPI (blue channel), EdU (green channel), and merge of DAPI and EdU. (E) Quantitation of the percentage of EdU^+ cells from three biologic replicates. Statistical significance of differences in means was determined with a paired Student t test ($P = 1.8 \times 10^{-3}$). (F) Intensity of fluorescence of nuclear EdU in induced or uninduced cells. Statistical significance of differences of distributions of data points from the two conditions was calculated with a Kolmogorov-Smirnov test ($P < 1 \times 10^{-15}$). (G) Distribution of trypanosome types after 18 hours of inducing knockdown of RPA1. Possible statistical significance of differences in distributions was calculated with a χ^2 test; $P = 2.84 \times 10^{-35}$. All statistical analysis was performed using Prism 9.0 (Graphpad). Horizontal lines represent means. Tet, tetracycline.

presented earlier (Fig. 8). CBL0137 addition to trypanosomes harboring these constructs led to loss of all three proteins (Supplemental Fig. 6C). Altogether, the data indicates that CBL0137 causes degradation of some but not all proteins. Further work is needed to examine this effect in detail.

CBL0137 Blocks Protein Synthesis. Our observation that CBL0137 reduces the abundance of several proteins (Fig. 8) led us to explore a possibility that the drug affected either degradation and/or synthesis of proteins. To distinguish between these possibilities, we examined the effect of CBL0137 on ribosomal

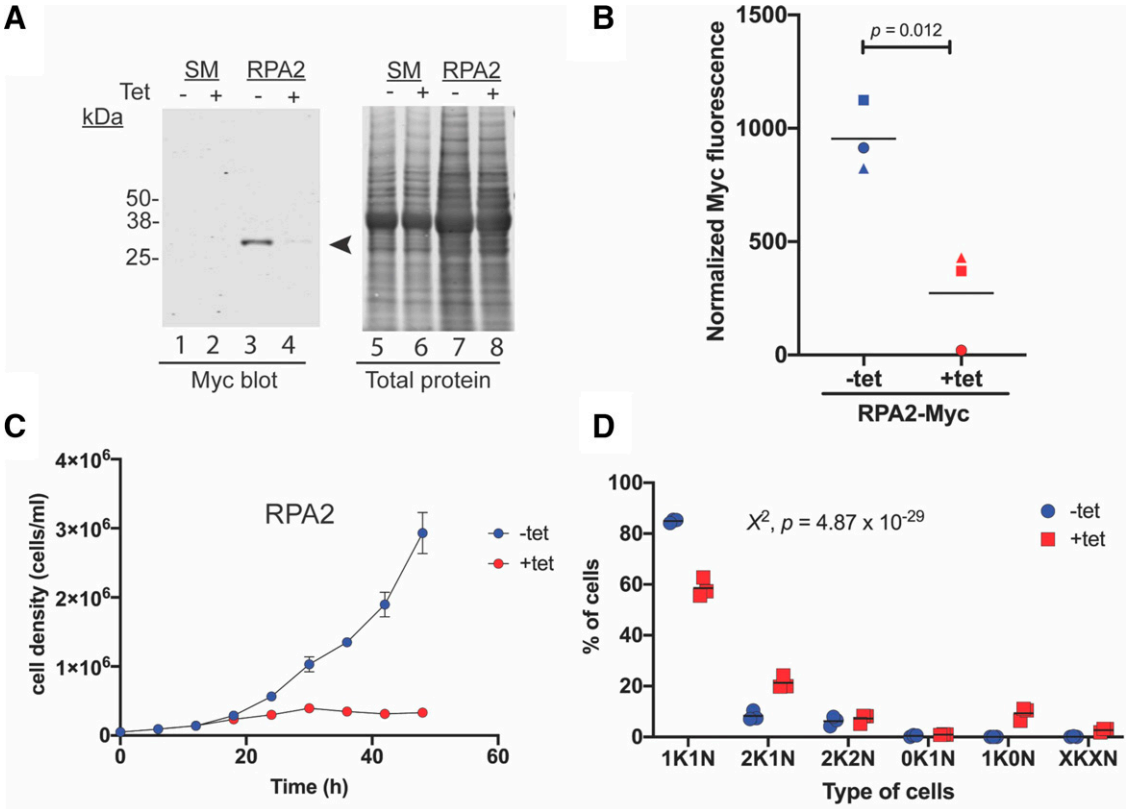

Fig. 6. RPA2 knockdown inhibits mitosis and produces anucleate trypanosomes. Trypanosomes expressing a c-terminus Myc-tagged RPA2 were transfected with an RNAi construct targeting RPA2. Stable transfectant clones were induced with tetracycline (1 μg/ml) for the different times indicated. (A) Western blot using 3×10^6 cells per lane of control (SM trypanosomes) and RPA2-Myc RNAi cell line. Primary antibody anti-Myc (9E10) rabbit monoclonal antibody (mAb)(Santa Cruz Biotech) was diluted 1:2500 in Intercept-PBS blocking solution (LI-COR) plus 0.2% of Tween-20. Secondary antibody was IRDye-800 anti-mouse (LI-COR) diluted 1:20000 (in Intercept-PBS, 0.2% of Tween-20, and 0.2% of SDS). (B) Quantitation of magnitude of change in RPA2-Myc between induced and uninduced trypanosomes from three biologic replicates. A paired Student *t* test was used to determine statistical significance of differences in mean values ($P = 0.012$). (C) Trypanosome proliferation-time course for RPA2 knockdown and controls. Three biologic replicates were studied, each with trypanosomes at a starting density of 1×10^5 cells per milliliter. Cultures were 10-fold to continue the study when density reached 1×10^6 trypanosomes per milliliter. (D) Distribution of different trypanosome types after 24-hour knockdown of RPA2. A χ^2 test using Prism 9.0 (Graphpad) was used to determine the possible statistical significance of differences in the distribution of cell types ($P = 4.87 \times 10^{-29}$). Horizontal lines represent means. Two RNAi cell lines for RPA2 were studied; they produced similar results. Tet, tetracycline.

protein synthesis, tracked by incorporation of a methionine analog HPG into polypeptides (Landgraf et al., 2015) (Fig. 9A).

Trypanosome polypeptides incorporate HPG (Fig. 9B, lane 2), and the process was blocked by cycloheximide, an inhibitor of eukaryote protein synthesis (Duszenko et al., 1999; Siegel et al., 2008) (Fig. 9B, lane 3). The effect of CBL0137 (180 nM (DCC_{25}), 290 nM (DCC_{50}), or 800 nM (DCC_{90}) on translation was assayed by a 15-minute preincubation of cells with drug followed by addition of HPG for 60 minutes (Fig. 9B, lane 4, lane 5, and lane 6). HPG incorporation into polypeptide was normalized to total protein content (Fig. 9B, lanes 7–12). CBL0137 inhibited translation at 290 nM (DCC_{50}) ($P = 3 \times 10^{-2}$) and 800 nM (DCC_{90}) ($P = 2 \times 10^{-3}$) but not at 180 nM (DCC_{25}) (Fig. 9C).

We surmise that CBL0137 inhibits translation of trypanosome proteins, an observation that helps explain reduction in steady-state amount of four proteins studied earlier (Fig. 8; Supplemental Fig. 6C). If new protein synthesis is inhibited by CBL0137 (Fig. 9), polypeptides with short half-lives may not be replenished when trypanosomes are treated with drug for 6 hours, leading to diminished steady-state levels in western blot assays (Fig. 8; Supplemental Fig. 6). Efficacy of CBL0137 against *T. brucei* in a mouse model of HAT (Thomas et al., 2016) most likely involves inhibition of protein synthesis, because plasma concentration of CBL0137 reaches 1.7 μM after oral administration of drug (40 mg/kg) (Sharma et al., manuscript in preparation). RPA1 knockdown, while copying some molecular effects of CBL0137, does not inhibit translation of proteins in *T. brucei* (Supplemental Fig. 5).

Discussion

From Binding Proteins to Physiologic Targets of Drugs. Implementation of "phenotypic screening" is on the rise in drug discovery projects for infectious, parasitic, oncologic, and chronic diseases (Chatelain and Ioset, 2018; Ferrins et al., 2018; Woodring et al., 2018; Bachovchin et al., 2019; Bryce et al., 2019; Buckner et al., 2020; Patra et al., 2020; Vincent et al., 2020; Warchal et al., 2020; Love and McNamara, 2021). Since targets of drugs discovered by phenotypic screening are unknown, an effort to find drug-binding proteins is a typical next step to understand mechanisms of action of the new drugs.

Although many pathways for drug target deconvolution are available, the most convincing ones use assays that are unbiased and monitor direct biochemical interactions between drugs and binding proteins (e.g., affinity chromatography and

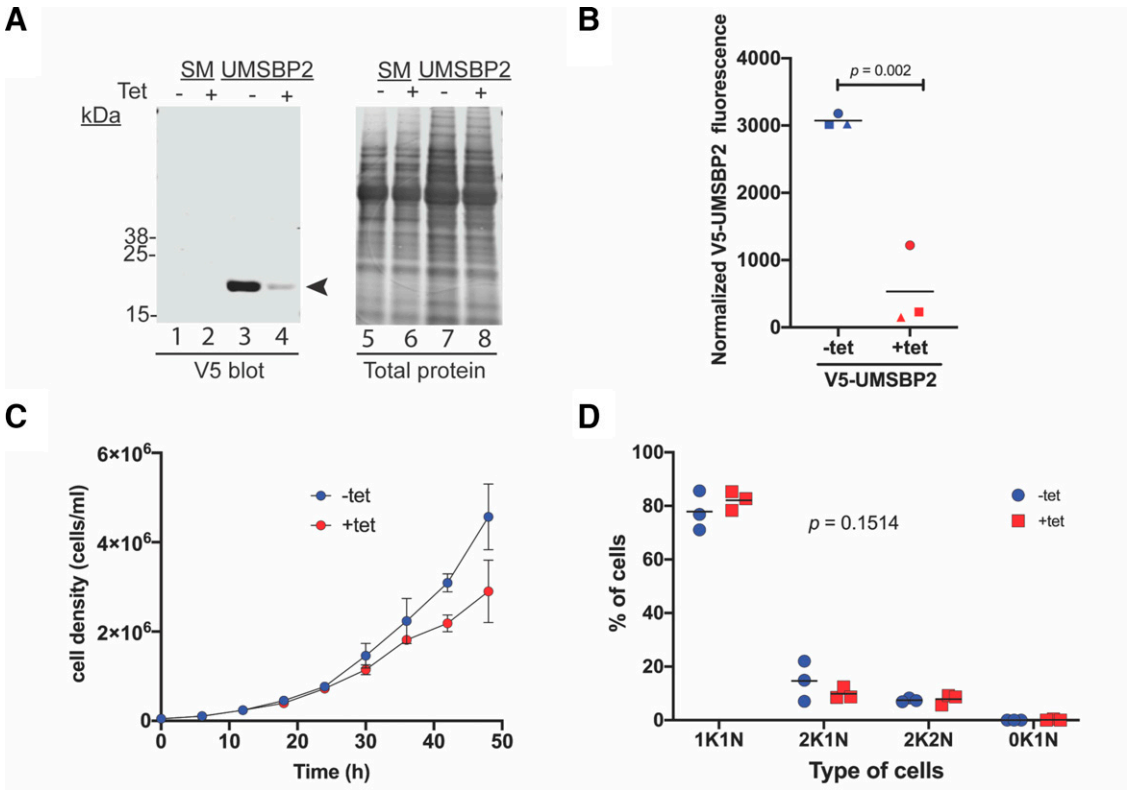

Fig. 7. UMSBP2 knockdown does not affect DNA replication or nucleus mitosis. Trypanosomes stably expressing a V5-tagged (at n-terminus) UMSBP2 were transfected with a UMSBP2 RNAi construct, and clonal lines selected *(Materials and Methods)*. RNAi was induced with tetracycline 1 μg/ml. (A) Western blot using 3×10^6 cells per lane of control (SM trypanosomes) or UMSBP2-RNAi trypanosome line induced for 24 hours. The primary antibody was anti-V5 (D3H8Q) rabbit mAb (Cell Signaling Technology) diluted 1:3000 [in Intercept-PBS blocking solution (Li-COR) plus 0.2% of tween-20]. Secondary antibody was IRDye-800 anti-rabbit (Li-COR) diluted 1:20000 (in Intercept-PBS, 0.2% of Tween-20, and 0.2% of SDS). (B) Quantitation of changes in V5-RPA1 protein level between induced and uninduced cells from three biologic replicates. A paired student *t* test was used to determine the possible statistical significance ($P = 0.002$) of differences in mean values. (C) Proliferation versus time curves for UMSBP2 knockdown or control trypanosomes. Cell were seeded at 1×10^5 cells per milliliter, and cell density was determined with a Coulter counter. Cultures reaching a density of 1×10^6 cells per milliliter were diluted 10-fold to continue the experiment. Three biologic replicates were obtained for each trypanosome line. (D) Distribution of different cell types after 24 hours of induction. A χ^2 test was used to calculate the possible significance of the differences in distribution of cell types ($P = 0.1514$). Two RNAi clonal lines for UMSBP2 were studied, and they produced very similar results. All statistical analysis was performed using Prism 9.0 (Graphpad). Tet, tetracycline.

photo-affinity labeling) (Rix et al., 2007; Shi et al., 2012; Franks and Hsu, 2019). Such direct strategies frequently yield tens of drug-binding proteins (Jones et al., 2015), creating a need to distinguish drug-binding proteins from physiologic targets of drugs. A "physiologic target of a drug" may be defined as a macromolecule whose knockdown or over-expression produces identical (or very similar) molecular effects as treatment of cells with the drug (Mensa-Wilmot, 2021). Many drug-binding proteins [for example, plasma proteins (Berezhkovskiy, 2008; Cho et al., 2010; Svennebring, 2016)] are not physiologic targets of the small molecules.

CBL0137-Binding Proteins and Molecular Modes of Action of the Drug. Fourteen CBL0137-binding proteins were identified with affinity chromatography (Table 1) and were used to predict molecular effects of CBL0137 on trypanosomes exposed to pharmacodynamically equivalent drug concentrations (DCC_{25}, for example) (Fig. 1).

CBL0137 inhibited nuclear (but not mitochondrial) DNA replication (Fig. 3), prevented nucleus mitosis (Fig. 4), and blocked polypeptide synthesis (Fig. 9). Despite identification of several glycolysis enzymes as drug-binding proteins (Table 1), CBL0137 failed to inhibit ATP synthesis (Supplemental Fig. 1), indicating that those enzymes are unlikely to be physiologic targets of the drug.

CBL0137 inhibition of polypeptide synthesis (Fig. 9) could explain pleiotropy of the drug's molecular effects. For example, blocking translation of proteins with short half-lives may be equivalent to a "loss of function" that leads to a specific molecular defect (e.g., inhibition of DNA synthesis). However, that hypothesis is undercut by the use of less drug to inhibit both DNA synthesis and mitosis than is needed to block translation (Fig. 9). Several antibacterial drugs act on ribosomal protein synthesis (reviewed in Lin et al., 2018). In trypanosomes, no inhibitors of protein synthesis are currently in development as drugs against the pathogen, although small molecules that inhibit methionyl-transfer RNA synthetase are being optimized (Huang et al., 2016; Zhang et al., 2020). To that end, CBL0137 represents a "first in class" lead drug with protein synthesis as a mode of action. CBL0137 is the first carbazole inhibitor of eukaryote protein synthesis.

In a previous study, a 24-hour treatment of *T. brucei* with 200 nM CBL0137 did not inhibit DNA synthesis (Thomas et al., 2016), apparently contradicting data presented in Fig. 3 of this work. In experiments to resolve this discrepancy, we found that in a 6-hour treatment of *T. brucei*, it requires 730 nM CBL0137 to inhibit DNA synthesis (Supplemental Fig. 2). A simple explanation for the observation is that a lower amount of CBL0137 slows down but does not terminate DNA synthesis, thereby

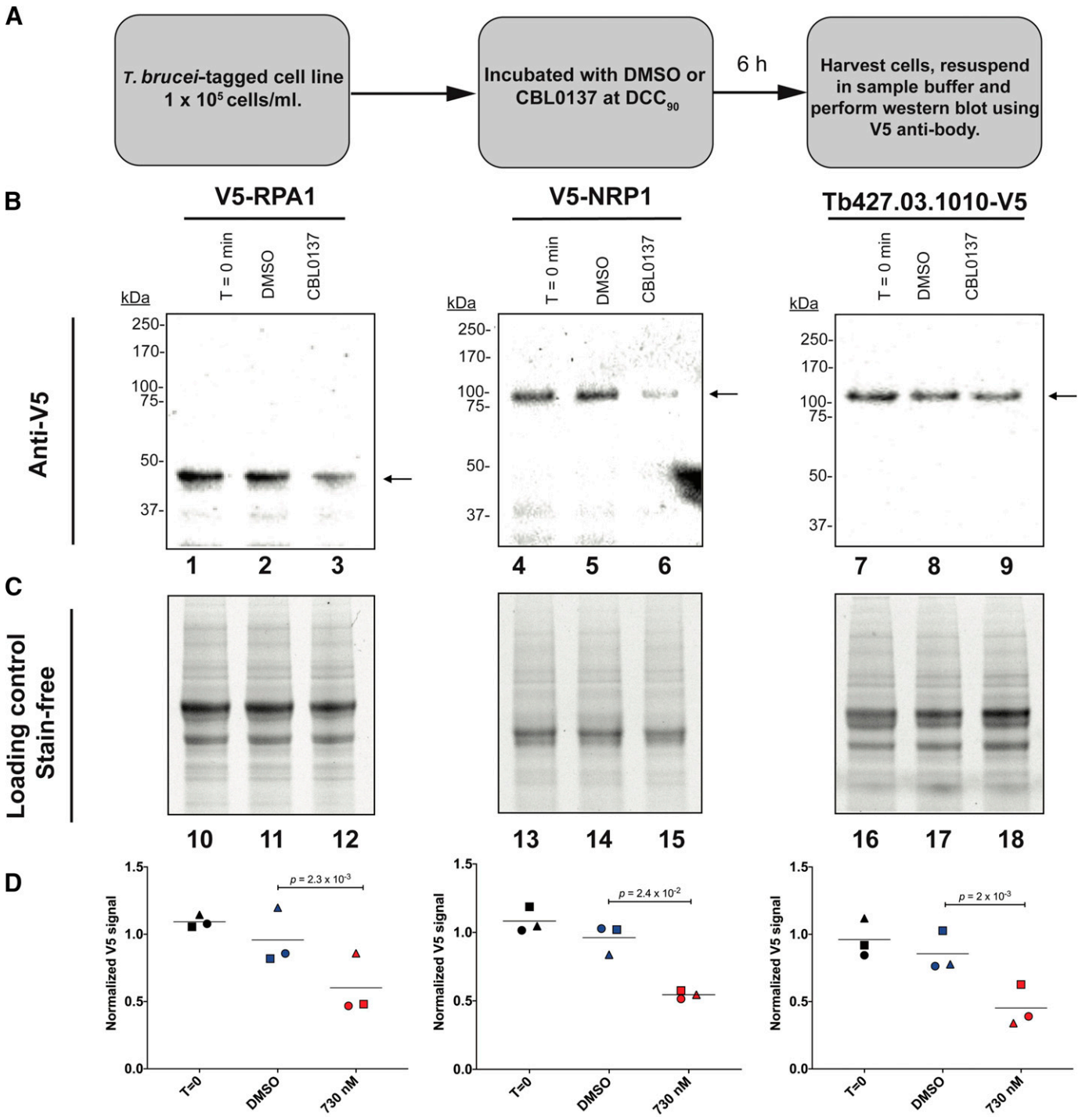

Fig. 8. CBL0137 alters proteostasis in the trypanosome. Clonal lines of *T. brucei* stably transfected with epitope-tagged forms of one of three proteins, namely V5-RPA1, V5-Tb427.tmp160.4770, and Tb427.03.1010-V5 were selected. (A) scheme of experimental procedure. Trypanosomes were inoculated at 1×10^5 cells per milliliter and incubated with or without DMSO, or CBL0137 (725 nM) for 6 hours. Cell lysates were electrophoresed and transferred to a PVDF membrane (Bio-Rad). Each lane (for electrophoresis) was loaded with 1×10^6 cell equivalents of lysate, except V5-RPA1, where 3×10^6 equivalents of lysate was used. Primary antibody was anti-V5 (D3H8Q) rabbit mAb (Cell Signaling) diluted 1:3000 in Tris base saline buffer (20 mM Tris, 150 mM NaCl) with 0.1% of Tween 20 at pH 8.0 (Tris-buffered saline with Tween). Secondary anti-rabbit antibody coupled to alkaline phosphatase (Bio-Rad) was diluted 1:3000 in Tris-buffered saline with Tween buffer and incubated with the membrane for 1 hour, after which the membrane was developed with an alkaline phosphatase reagent (Bio-Rad). The experiment was performed three times with different biologic samples. (B) A representative western blot for each tagged protein is presented with the arrow pointing to the anti-V5 signal. (C) Loading control image of a stain-free gel detected using ChemiDoc XRS+ (Bio-Rad). (D) Normalized quantitation for three biologic replicates of each experiment. For normalization, the anti-V5 signal was corrected for total protein in the entire lane. A paired student *t* test was used to determine statistical significance in means of the data from the three biologic replicates (*P* values between DMSO control and treated samples were 2.3×10^{-3}, 2.4×10^{-3}, and 2×10^{-3} for V5-RPA1, V5-NRP1, and Tb427.03.1010-V5, respectively). Statistical analysis was performed using Prism 9.0 (Graphpad). Horizontal lines represent means.

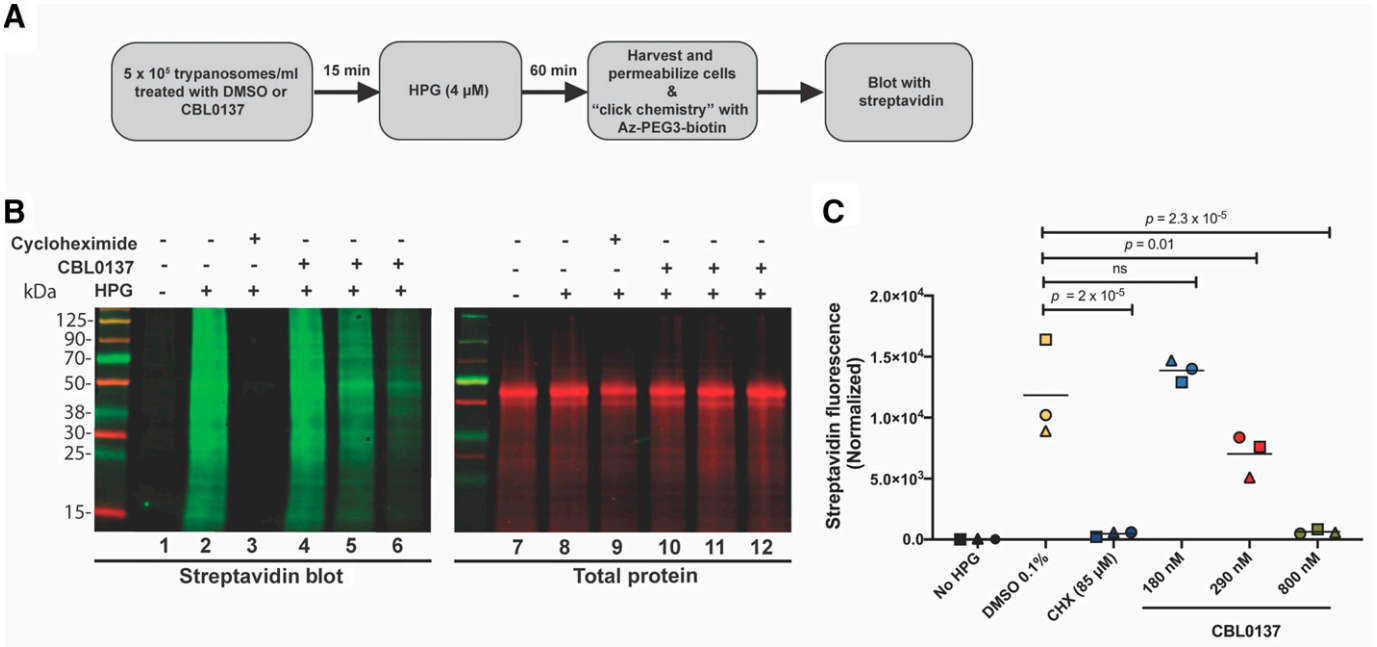

Fig. 9. CBL0137 inhibits protein synthesis. (A) Scheme of the experimental protocol. *T. brucei* (5×10^5 cell/ml) was incubated with DMSO (0.1%) or different concentrations of CBL0137 for 15 minutes before HPG addition and "click chemistry" with azide-PEG3-biotin. Cycloheximide was added at DCC_{90} concentration (85 μM) as a positive control. (B) A representative western blot (1×10^6 cell equivalents of lysate per lane) probed with IRDye-streptavidin 800 CW (1:2500 dilution) (LI-COR). Total protein was tracked using REVERT protein stain (Li-COR). Images were captured using Odyssey CLx (LI-COR) and data processed using Image Studio Lite Quantitation Software v 5.2.5 (LI-COR). (C) Quantitation of CBL0137 effects on nascent polypeptide synthesis. Total protein from each lane (lane 7 to lane 12) was used as a correction factor for HPG incorporation in each lane (lane 2 to lane 6) (i.e., normalized streptavidin fluorescence). Three biologic replicates were tested. A paired two-sided student *t* test (Prism 9.0, GraphPad) was used to compare differences in means of normalized fluorescence intensities between DMSO (control) and cycloheximide or CBL0137-treated trypanosomes. Horizontal lines denote means. ns, not significant.

permitting DNA replication over a long period of time. Curiously, the higher concentration of drug needed to inhibit DNA synthesis is exceeded in mice after oral dosing (60 mg/kg) of CBL0137 (Sharma et al., manuscript in preparation). Therefore, it seems possible that the trypanocidal effect of CBL0137 in mice involves inhibition of nuclear DNA synthesis.

Polypharmacology of CBL0137 (i.e., inhibition of DNA replication, mitosis, and protein synthesis at concentrations above 290 nM) (Fig. 10) bodes well for using it as an antitrypanosome drug. Interaction with two or more targets suggests that it might be difficult for trypanosomes to develop resistance after chemotherapy with CBL0137.

Physiologic Targets Explain Modes of Action of CBL0137. We used affinity chromatography, as an unbiased approach, to identify fourteen CBL0137-binding proteins (Table 1). These CBL0137-binding proteins may seem unique when compared with the data from human cells, where the drug interferes with aspects of chromatin biology (Sergeev et al., 2020; Dallavalle et al., 2021; Lu et al., 2021). However, no CBL0137-binding proteins have been identified with an unbiased biochemical strategy in human cells. Therefore, one cannot directly compare our data with information from human cells.

In pursuit of physiologic targets of the drug, trypanosome genes encoding CBL0137-binding proteins were knocked down, and resulting molecular effects were compared with those obtained after perturbation of trypanosomes with the drug (Meyer and Shapiro, 2021). For physiologic targets of the drug, the expectation was that molecular defects determined after their knockdown would be very similar to those obtained after adding CBL0137 to trypanosomes (Mensa-Wilmot, 2021).

Data obtained for RPA1 and RPA2 is consistent with their designation as physiologic targets of CBL0137. Knockdown of that RPA1 inhibited DNA replication, and prevented mitosis, like effects observed after adding CBL0137 to trypanosomes. RPA2, expected to form a complex with RPA1 in vivo (Maniar et al., 1997; Chen and Wold, 2014), yielded data after RNAi that are in line with designation as a physiologic target by inhibiting mitosis (Fig. 6D). That knockdown of RPA1 and RPA2 did not produce identical results in *T. brucei* is not completely surprising since divergence of the functions of RPA1 and RPA2 has been noted in *Arabidopsis thaliana* and in *Caenorhabditis elegans* (Hefel et al., 2021).

Involvement of RPA1 in mitosis is novel. In other organisms, homologs of the protein in complex with RPA2 and RPA3 participate in aspects of DNA synthesis, repair, and recombination (Caldwell and Spies, 2020; Chowdhury et al., 2021). However, there are no reports yet of a role in mitosis. In future work, analysis of the binding partners of trypanosome RPA1 may shed light on how the protein contributes to mitosis.

Further work is needed to identify other physiologic targets of CBL0137. We do not know proteins whose interaction with CBL0137 inhibits translation of mRNAs (Fig. 9). Our affinity chromatography work produced four RNA-binding proteins, namely poly(A)-binding protein 2, an ALBA-domain protein, RNA-binding protein DRBD2, and RNA-binding protein DRBD3 as CBL0137-binding proteins (Table 1). These genes will be a good starting point to

A

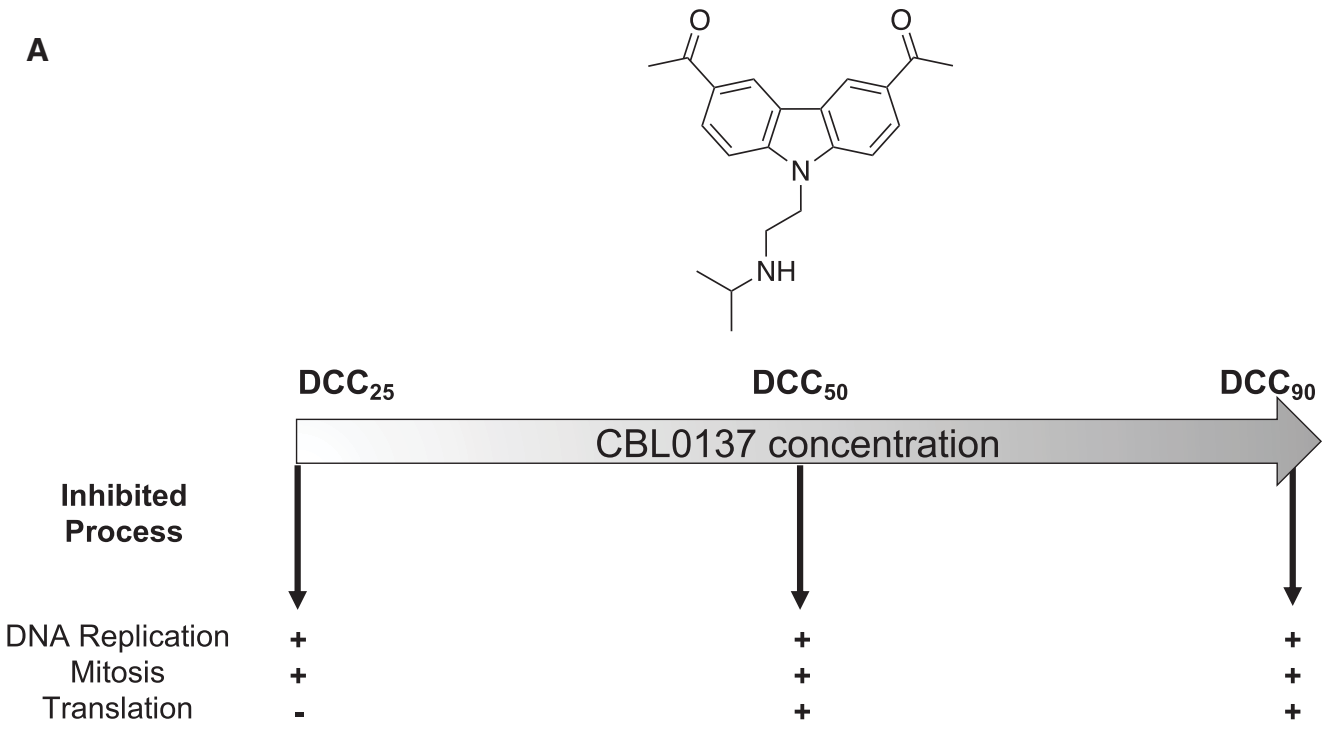

B

Gene	Mitosis Inhibition	DNA Replication Inhibition	Translation Inhibition	XK1N Present	1K0N Present
RPA1	YES	YES	NO	YES	NO
RPA2	YES	ND	ND	NO	YES
UMSBP2	NO	ND	ND	NO	NO

Fig. 10. Summary of molecular modes of CBL0137 action. (A) Molecular effects of CBL0137 on three pathways are listed below the arrows, with + indicating inhibitory effect and – for no effect. At DCC_{25}, CBL0137 inhibits DNA replication and mitosis, and at DCC_{50}, the drug also blocks protein synthesis. (B) Effect of knockdown of CBL0137-binding proteins on mitosis, DNA replication, polypeptide translation, and emergence of XK1N (multikinetoplasts, one nucleus) or 1K0N trypanosomes.

discover physiologic targets of CBL0137 that regulate protein synthesis in the African trypanosome.

Authorship Contributions

Participated in research design: Sanz-Rodríguez, Guyett, Mensa-Wilmot.

Conducted experiments: Sanz-Rodríguez, Hoffman.

Contributed new reagents or analytic tools: Guyett, Singh, Pollastri.

Performed data analysis: Sanz-Rodríguez, Hoffman, Mensa-Wilmot.

Wrote or contributed to the writing of the manuscript: Hoffman, Purmal, Pollastri, Mensa-Wilmot.

References

Abo-Rady M, Bellmann J, Glatza M, Marrone L, Reinhardt L, Tena S, and Sterneckert J (2019) Phenotypic Screening Using Mouse and Human Stem Cell-Based Models of Neuroinflammation and Gene Expression Analysis to Study Drug Responses. *Methods Mol Biol* **1888**:21–43.

Andre J, Kerry L, Qi X, Hawkins E, Drizyte K, Ginger ML, and McKean PG (2014) An alternative model for the role of RP2 protein in flagellum assembly in the African trypanosome. *J Biol Chem* **289**:464–475.

Bachovchin KA, Sharma A, Bag S, Klug DM, Schneider KM, Singh B, Jalani HB, Buskes MJ, Mehta N, Tanghe S, et al. (2019) Improvement of Aqueous Solubility of Lapatinib-Derived Analogues: Identification of a Quinolinimine Lead for Human African Trypanosomiasis Drug Development. *J Med Chem* **62**:665–687.

Berezhkovskiy LM (2008) Some features of the kinetics and equilibrium of drug binding to plasma proteins. *Expert Opin Drug Metab Toxicol* **4**:1479–1498.

Bochkarev A, Bochkareva E, Frappier L, and Edwards AM (1999) The crystal structure of the complex of replication protein A subunits RPA32 and RPA14 reveals a mechanism for single-stranded DNA binding. *EMBO J* **18**:4498–4504.

Braun KA, Lao Y, He Z, Ingles CJ, and Wold MS (1997) Role of protein-protein interactions in the function of replication protein A (RPA): RPA modulates the activity of DNA polymerase alpha by multiple mechanisms. *Biochemistry* **36**: 8443–8454.

Brown SV, Hosking P, Li J, and Williams N (2006) ATP synthase is responsible for maintaining mitochondrial membrane potential in bloodstream form Trypanosoma brucei. *Eukaryot Cell* **5**:45–53.

Bryce NS, Hardeman EC, Gunning PW, and Lock JG (2019) Chemical biology approaches targeting the actin cytoskeleton through phenotypic screening. *Curr Opin Chem Biol* **51**:40–47.

Buckner FS, Buchynskyy A, Nagendar P, Patrick DA, Gillespie JR, Herbst Z, Tidwell RR, and Gelb MH (2020) Phenotypic Drug Discovery for Human African Trypanosomiasis: A Powerful Approach. *Trop Med Infect Dis* **5**:23.

Butera JA (2013) Phenotypic screening as a strategic component of drug discovery programs targeting novel antiparasitic and antimycobacterial agents: an editorial. *J Med Chem* **56**:7715–7718.

Caldwell CC and Spies M (2020) Dynamic elements of replication protein A at the crossroads of DNA replication, recombination, and repair. *Crit Rev Biochem Mol Biol* **55**:482–507.

Chatelain E and Ioset JR (2018) Phenotypic screening approaches for Chagas disease drug discovery. *Expert Opin Drug Discov* **13**:141–153.

Chen R and Wold MS (2014) Replication protein A: single-stranded DNA's first responder: dynamic DNA-interactions allow replication protein A to direct single-strand DNA intermediates into different pathways for synthesis or repair. *BioEssays* **36**:1156–1161.

Cho SY, Ohnuma T, Silverman LR, Holland JF, and Roboz J (2010) Discontinuous drug binding to proteins: binding of an antineoplastic benzyl styryl sulfone to albumin and enzymes in vitro and in phase I clinical trials. *Drug Metab Dispos* **38**:1480–1485.

Chowdhury S, Chowdhury AB, Kumar M, and Chakraborty S (2021) Revisiting regulatory roles of replication protein A in plant DNA metabolism. *Planta* **253**:130.

Dallavalle S, Mattio LM, Artali R, Musso L, Aviñó A, Fàbrega C, Eritja R, Gargallo R, and Mazzini S (2021) Exploring the Interaction of Curaxin CBL0137 with G-Quadruplex DNA Oligomers. *Int J Mol Sci* **22**:6476.

Drowley L, McPheat J, Nordqvist A, Peel S, Karlsson U, Martinsson S, Müllers E, Dellsén A, Knight S, Barrett I et al. (2020) Discovery of retinoic acid receptor agonists as proliferators of cardiac progenitor cells through a phenotypic screening approach. *Stem Cells Transl Med* **9**:47–60.

Duszenko M, Kang X, Böhme U, Hömke R, and Lehner M (1999) In vitro translation in a cell-free system from Trypanosoma brucei yields glycosylated and glycosylphosphatidylinositol-anchored proteins. *Eur J Biochem* **266**:789–797.

Eng JK, McCormack AL, and Yates JR (1994) An approach to correlate tandem mass spectral data of peptides with amino acid sequences in a protein database. *J Am Soc Mass Spectrom* **5**:976–989.

Erdile LF, Heyer WD, Kolodner R, and Kelly TJ (1991) Characterization of a cDNA encoding the 70-kDa single-stranded DNA-binding subunit of human replication protein A and the role of the protein in DNA replication. *J Biol Chem* **266**:12090–12098.

Ferguson L, Wells G, Bhakta S, Johnson J, Guzman J, Parish T, Prentice RA, and Brucoli F (2019) Integrated Target-Based and Phenotypic Screening Approaches for the Identification of Anti-Tubercular Agents That Bind to the Mycobacterial Adenylating Enzyme MbtA. *ChemMedChem* **14**:1735–1741.

Ferrins L, Sharma A, Thomas SM, Mehta N, Erath J, Tanghe S, Leed SE, Rodriguez A, Mensa-Wilmot K, Sciotti RJ, et al. (2018) Anilinoquinoline based inhibitors of trypanosomatid proliferation. *PLoS Negl Trop Dis* **12**:e0006834.

Franks CE and Hsu KL (2019) Activity-Based Kinome Profiling Using Chemical Proteomics and ATP Acyl Phosphates. *Curr Protoc Chem Biol* **11**:e72.

Gilda JE and Gomes AV (2015) Western blotting using in-gel protein labeling as a normalization control: stain-free technology. *Methods Mol Biol* **1295**:381–391.

Glover L, Marques CA, Suska O, and Horn D (2019) Persistent DNA Damage Foci and DNA Replication with a Broken Chromosome in the African Trypanosome. *MBio* **10**:e01252-19.

Gürtler A, Kunz N, Gomolka M, Hornhardt S, Friedl AA, McDonald K, Kohn JE, and Posch A (2013) Stain-Free technology as a normalization tool in Western blot analysis. *Anal Biochem* **433**:105–111.

Guyett PJ, Xia S, Swinney DC, Pollastri MP, and Mensa-Wilmot K (2016) Glycogen Synthase Kinase 3β Promotes the Endocytosis of Transferrin in the African Trypanosome. *ACS Infect Dis* **2**:518–528.

Han JJ, Song ZT, Sun JL, Yang ZT, Xian MJ, Wang S, Sun L, and Liu JX (2018) Chromatin remodeling factor CHR18 interacts with replication protein RPA1A to regulate the DNA replication stress response in Arabidopsis. *New Phytol* **220**:476–487.

Haring SJ, Mason AC, Binz SK, and Wold MS (2008) Cellular functions of human RPA1. Multiple roles of domains in replication, repair, and checkpoints. *J Biol Chem* **283**:19095–19111.

Hefel A, Honda M, Cronin N, Harrell K, Patel P, Spies M, and Smolikove S (2021) RPA complexes in Caenorhabditis elegans meiosis; unique roles in replication, meiotic recombination and apoptosis. *Nucleic Acids Res* **49**:2005–2026.

Hirumi H and Hirumi K (1989) Continuous cultivation of Trypanosoma brucei blood stream forms in a medium containing a low concentration of serum protein without feeder cell layers. *J Parasitol* **75**:985–989.

Huang W, Zhang Z, Barros-Álvarez X, Koh CY, Ranade RM, Gillespie JR, Creason SA, Shibata S, Verlinde CLMJ, Hol WGJ, et al. (2016) Structure-guided design of novel Trypanosoma brucei Methionyl-tRNA synthetase inhibitors. *Eur J Med Chem* **124**:1081–1092.

Jacobs RT, Plattner JJ, Nare B, Wring SA, Chen D, Freund Y, Gaukel EG, Orr MD, Perales JB, Jenks M, et al. (2011) Benzoxaboroles: a new class of potential drugs for human African trypanosomiasis. *Future Med Chem* **3**:1259–1278.

Jensen RE and Englund PT (2012) Network news: the replication of kinetoplast DNA. *Annu Rev Microbiol* **66**:473–491.

Jones DC, Foth BJ, Urbaniak MD, Patterson S, Ong HB, Berriman M, and Fairlamb AH (2015) Genomic and Proteomic Studies on the Mode of Action of Oxaboroles against the African Trypanosome. *PLoS Negl Trop Dis* **9**:e0004299.

Kaiser M, Bray MA, Cal M, Bourdin Trunz B, Torreele E, and Brun R (2011) Antitrypanosomal activity of fexinidazole, a new oral nitroimidazole drug candidate for treatment of sleeping sickness. *Antimicrob Agents Chemother* **55**:5602–5608.

Käll L, Canterbury JD, Weston J, Noble WS, and MacCoss MJ (2007) Semi-supervised learning for peptide identification from shotgun proteomics datasets. *Nat Methods* **4**:923–925.

Käll L, Storey JD, and Noble WS (2008) Non-parametric estimation of posterior error probabilities associated with peptides identified by tandem mass spectrometry. *Bioinformatics* **24**:i42–i48.

Käll L, Storey JD, and Noble WS (2009) QVALITY: non-parametric estimation of q-values and posterior error probabilities. *Bioinformatics* **25**:964–966.

Keatinge M, Tsarouchas TM, Munir T, Porter NJ, Larraz J, Gianni D, Tsai HH, Becker CG, Lyons DA, and Becker T (2021) CRISPR gRNA phenotypic screening in zebrafish reveals pro-regenerative genes in spinal cord injury. *PLoS Genet* **17**:e1009515.

Kim HS and Brill SJ (2001) Rfc4 interacts with Rpa1 and is required for both DNA replication and DNA damage checkpoints in Saccharomyces cerevisiae. *Mol Cell Biol* **21**:3725–3737.

Klebanov-Akopyan O, Mishra A, Glousker G, Tzfati Y, and Shlomai J (2018) Trypanosoma brucei UMSBP2 is a single-stranded telomeric DNA binding protein essential for chromosome end protection. *Nucleic Acids Res* **46**:7757–7771.

Koman IE, Commane M, Paszkiewicz G, Hoonjan B, Pal S, Safina A, Toshkov I, Purmal AA, Wang D, Liu S, et al. (2012) Targeting FACT complex suppresses mammary tumorigenesis in Her2/neu transgenic mice. *Cancer Prev Res (Phila)* **5**:1025–1035.

Landgraf P, Antileo ER, Schuman EM, and Dieterich DC (2015) BONCAT: metabolic labeling, click chemistry, and affinity purification of newly synthesized proteomes. *Methods Mol Biol* **1266**:199–215.

Lin J, Zhou D, Steitz TA, Polikanov YS, and Gagnon MG (2018) Ribosome-Targeting Antibiotics: Modes of Action, Mechanisms of Resistance, and Implications for Drug Design. *Annu Rev Biochem* **87**:451–478.

Lindner AK, Lejon V, Chappuis F, Seixas J, Kazumba L, Barrett MP, Mwamba E, Erphas O, Akl EA, Villanueva G, et al. (2020) New WHO guidelines for treatment of gambiense human African trypanosomiasis including fexinidazole: substantial changes for clinical practice. *Lancet Infect Dis* **20**:e38–e46.

Love MS and McNamara CW (2021) Phenotypic screening techniques for *Cryptosporidium* drug discovery. *Expert Opin Drug Discov* **16**:59–74.

Lu K, Liu C, Liu Y, Luo A, Chen J, Lei Z, Kong J, Xiao X, Zhang S, Wang YZ, et al. (2021) Curaxin-Induced DNA Topology Alterations Trigger the Distinct Binding Response of CTCF and FACT at the Single-Molecule Level. *Biochemistry* **60**:494–499.

Maniar HS, Wilson R, and Brill SJ (1997) Roles of replication protein-A subunits 2 and 3 in DNA replication fork movement in Saccharomyces cerevisiae. *Genetics* **145**:891–902.

McQuin C, Goodman A, Chernyshev V, Kamentsky L, Cimini BA, Karhohs KW, Doan M, Ding L, Rafelski SM, Thirstrup D, et al. (2018) CellProfiler 3.0: Next-generation image processing for biology. *PLoS Biol* **16**:e2005970.

Mensa-Wilmot K (2021) How Physiologic Targets Can Be Distinguished from Drug-Binding Proteins. *Mol Pharmacol* **100**:1–6.

Meyer KJ and Shapiro TA (2021) Cytosolic and Mitochondrial Hsp90 in Cytokinesis, Mitochondrial DNA Replication, and Drug Action in Trypanosoma brucei. *Antimicrob Agents Chemother* **65**:e0063221.

Milman N, Motyka SA, Englund PT, Robinson D, and Shlomai J (2007) Mitochondrial origin-binding protein UMSBP mediates DNA replication and segregation in trypanosomes. *Proc Natl Acad Sci USA* **104**:19250–19255.

Mondal A and Bhattacherjee A (2020) Mechanism of Dynamic Binding of Replication Protein A to ssDNA. *J Chem Inf Model* **60**:5057–5069.

Olson E, Nievera CJ, Klimovich V, Fanning E, and Wu X (2006) RPA2 is a direct downstream target for ATR to regulate the S-phase checkpoint. *J Biol Chem* **281**:39517–39533.

Orsburn BC (2021) Proteome Discoverer-A Community Enhanced Data Processing Suite for Protein Informatics. *Proteomes* **9**:15.

Palomba A, Abbondio M, Fiorito G, Uzzau S, Pagnozzi D, and Tanca A (2021) Comparative Evaluation of MaxQuant and Proteome Discoverer MS1-Based Protein Quantification Tools. *J Proteome Res* **20**:3497–3507.

Patra AT, Hingamire T, Belekar MA, Xiong A, Subramanian G, Bozdech Z, Preiser P, Shanmugam D, and Chandramohanadas R (2020) Whole-Cell Phenotypic Screening of Medicines for Malaria Venture Pathogen Box Identifies Specific Inhibitors of *Plasmodium falciparum* Late-Stage Development and Egress. *Antimicrob Agents Chemother* **64**:e01802-19.

Pelfrene E, Harvey Allchurch M, Ntamabyaliro N, Nambasa V, Ventura FV, Nagercoil N, and Cavaleri M (2019) The European Medicines Agency's scientific opinion on oral fexinidazole for human African trypanosomiasis. *PLoS Negl Trop Dis* **13**:e0007381.

Pollastri MP (2018) Fexinidazole: a new drug for African sleeping sickness on the horizon. *Trends Parasitol* **34**:178–179.

Povelones ML (2014) Beyond replication: division and segregation of mitochondrial DNA in kinetoplastids. *Mol Biochem Parasitol* **196**:53–60.

Punna S, Kaltgrad E, and Finn MG (2005) "Clickable" agarose for affinity chromatography. *Bioconjug Chem* **16**:1536–1541.

Rix U, Hantschel O, Dürnberger G, Remsing Rix LL, Planyavsky M, Fernbach NV, Kaupe I, Bennett KL, Valent P, Colinge J, et al. (2007) Chemical proteomic profiles of the BCR-ABL inhibitors imatinib, nilotinib, and dasatinib reveal novel kinase and nonkinase targets. *Blood* **110**:4055–4063.

Rostovtsev VV, Green LG, Fokin VV, and Sharpless KB (2002) A stepwise huisgen cycloaddition process: copper(I)-catalyzed regioselective "ligation" of azides and terminal alkynes. *Angew Chem Int Ed Engl* **41**:2596–2599.

Ruillier V, Tournois J, Boissart C, Lasbareilles M, Mahé G, Chatrousse L, Cailleret M, Peschanski M, and Benchoua A (2020) Rescuing compounds for Lesch-Nyhan disease identified using stem cell-based phenotypic screening. *JCI Insight* **5**:e132094.

Schnaufer A, Clark-Walker GD, Steinberg AG, and Stuart K (2005) The F1-ATP synthase complex in bloodstream stage trypanosomes has an unusual and essential function. *EMBO J* **24**:4029–4040.

Sergeev A, Vorobyov A, Yakubovskaya M, Kirsanova O, and Gromova E (2020) Novel anticancer drug curaxin CBL0137 impairs DNA methylation by eukaryotic DNA methyltransferase Dnmt3a. *Bioorg Med Chem Lett* **30**:127296.

Shapovalov V, Kopanitsa L, Pruteanu LL, Ladds G, and Bailey DS (2021) Transcriptomics-Based Phenotypic Screening Supports Drug Discovery in Human Glioblastoma Cells. *Cancers (Basel)* **13**:3780.

Shen S, Arhin GK, Ullu E, and Tschudi C (2001) In vivo epitope tagging of Trypanosoma brucei genes using a one step PCR-based strategy. *Mol Biochem Parasitol* **113**:171–173.

Shi H, Zhang CJ, Chen GY, and Yao SQ (2012) Cell-based proteome profiling of potential dasatinib targets by use of affinity-based probes. *J Am Chem Soc* **134**:3001–3014.
Siegel TN, Kawahara T, Degrasse JA, Janzen CJ, Horn D, and Cross GA (2008) Acetylation of histone H4K4 is cell cycle regulated and mediated by HAT3 in Trypanosoma brucei. *Mol Microbiol* **67**:762–771.
Sokolova AY, Wyllie S, Patterson S, Oza SL, Read KD, and Fairlamb AH (2010) Cross-resistance to nitro drugs and implications for treatment of human African trypanosomiasis. *Antimicrob Agents Chemother* **54**:2893–2900.
Soliman K (2015) CellProfiler: Novel Automated Image Segmentation Procedure for Super-Resolution Microscopy. *Biol Proced Online* **17**:11.
Sullenberger C, Piqué D, Ogata Y, and Mensa-Wilmot K (2017) AEE788 Inhibits Basal Body Assembly and Blocks DNA Replication in the African Trypanosome. *Mol Pharmacol* **91**:482–498.
Svennebring AM (2016) The impact of the concentration of drug binding plasma proteins on drug distribution according to Øie-Tozer's model. *Xenobiotica* **46**:307–314.
Swalley SE (2020) Expanding therapeutic opportunities for neurodegenerative diseases: A perspective on the important role of phenotypic screening. *Bioorg Med Chem* **28**:115239.
Swinney DC and Anthony J (2011) How were new medicines discovered? *Nat Rev Drug Discov* **10**:507–519.
Thomas SM, Purmal A, Pollastri M, and Mensa-Wilmot K (2016) Discovery of a Carbazole-Derived Lead Drug for Human African Trypanosomiasis. *Sci Rep* **6**:32083.
Torreele E, Bourdin Trunz B, Tweats D, Kaiser M, Brun R, Mazué G, Bray MA, and Pécoul B (2010) Fexinidazole–a new oral nitroimidazole drug candidate entering clinical development for the treatment of sleeping sickness. *PLoS Negl Trop Dis* **4**:e923.
van Weelden SW, Fast B, Vogt A, van der Meer P, Saas J, van Hellemond JJ, Tielens AG, and Boshart M (2003) Procyclic Trypanosoma brucei do not use Krebs cycle activity for energy generation. *J Biol Chem* **278**:12854–12863.
Vincent F, Loria PM, Weston AD, Steppan CM, Doyonnas R, Wang YM, Rockwell KL, and Peakman MC (2020) Hit Triage and Validation in Phenotypic Screening: Considerations and Strategies. *Cell Chem Biol* **27**:1332–1346.
Wang F, Zhao Q, Liu J, Wang Z, and Kong D (2020) Identification of human lactate dehydrogenase A inhibitors with anti-osteosarcoma activity through cell-based phenotypic screening. *Bioorg Med Chem Lett* **30**:126909.
Warchal SJ, Dawson JC, Shepherd E, Munro AF, Hughes RE, Makda A, and Carragher NO (2020) High content phenotypic screening identifies serotonin receptor modulators with selective activity upon breast cancer cell cycle and cytokine signaling pathways. *Bioorg Med Chem* **28**:115209.
Watson JA, Strub-Wourgraft N, Tarral A, Ribeiro I, Tarning J, and White NJ (2019) Pharmacokinetic-Pharmacodynamic Assessment of the Hepatic and Bone Marrow Toxicities of the New Trypanoside Fexinidazole. *Antimicrob Agents Chemother* **63**:e02515-18.
Weng Q, Che J, Zhang Z, Zheng J, Zhan W, Lin S, Tian T, Wang J, Gai R, Hu Y, et al. (2019) Phenotypic Screening-Based Identification of 3,4-Disubstituted Piperidine Derivatives as Macrophage M2 Polarization Modulators: An Opportunity for Treating Multiple Sclerosis. *J Med Chem* **62**:3268–3285.
Wirtz E, Leal S, Ochatt C, and Cross GA (1999) A tightly regulated inducible expression system for conditional gene knock-outs and dominant-negative genetics in Trypanosoma brucei. *Mol Biochem Parasitol* **99**:89–101.
Wold MS (1997) Replication protein A: a heterotrimeric, single-stranded DNA-binding protein required for eukaryotic DNA metabolism. *Annu Rev Biochem* **66**:61–92.
Woodring JL, Behera R, Sharma A, Wiedeman J, Patel G, Singh B, Guyett P, Amata E, Erath J, Roncal N, et al. (2018) Series of Alkynyl-Substituted Thienopyrimidines as Inhibitors of Protozoan Parasite Proliferation. *ACS Med Chem Lett* **9**:996–1001.
Zhang Z, Barros-Álvarez X, Gillespie JR, Ranade RM, Huang W, Shibata S, Molasky NMR, Faghih O, Mushtaq A, Choy RKM, et al. (2020) Structure-guided discovery of selective methionyl-tRNA synthetase inhibitors with potent activity against *Trypanosoma brucei*. *RSC Med Chem* **11**:885–895.

Address correspondence to: Dr. Kojo Mensa-Wilmot, Department of Molecular and Cellular Biology, Kennesaw State University, 105 Marietta Drive, Room 5016, MailDrop 1301, Kennesaw, GA 30144. E-mail: kmensawi@kennesaw.edu